White paper on Proposed Ground-motion Prediction Equations (GMPEs) for 2015 National Seismic Hazard Maps

Final Version, Nov. 2012

Gail Atkinson, with input from John Adams, Garry Rogers, Tuna Onur and Karen Assatourians

Executive Summary

This is a set of working notes that describes the proposed GMPEs for use in the 2015 NBCC seismic hazard maps. The notes are "evolutionary" in that an initial proposal was developed, modified through feedback, then further modified to account for review suggestions (from Paul Somerville) regarding preferred ground-motion equations to consider. The main body of the notes describes the initial proposal and how it was re-worked to include epistemic uncertainty. Appendix B describes changes made to the suite and its weights to reflect review comments. The basic concept is that alternative GMPEs and data are used to specify a central, upper and lower representative equation set for each region/event type. The alternative equations express epistemic uncertainty in the correct median equations. Aleatory variability (scatter) is described separately, and is considered common to all models. All GMPEs are for B/C boundary site conditions. The final recommended GMPEs are posted in tabular format at www.seismotoolbox.ca.

Introduction

This is a discussion document that outlines proposed GMPEs for use in the 2015 NBCC seismic hazard maps. The document reflects evolving recommendations based on ongoing discussions with the NBCC ground-motion development group listed above. This document summarizes the final recommendations, which were arrived at by starting with an initial suite (as described in the body of this report and Appendix A), then modifying the suite in light of review comments received from the SCED External Reviewer, Paul Somerville; the modifications and their rationale are described in Appendix B. The median GMPEs are discussed separately from the issue of the appropriate 'sigma' (standard deviation about the median), which follows the discussion of the median equations. The GMPEs (and sigma) are important input parameters to the seismic hazard mapping software being used to develop and test the maps (modified FRISK88 program of McGuire, Toro et al. being used by the GSC, and EQHaz program of Assatourians and Atkinson being used at Western). The GMPEs need to be updated from those used in the last hazard maps, to reflect the last 15 years of developments in the ground-motion field; during this time period, the databases on which GMPEs are based have grown manifold, and thus the changes in knowledge have been significant.

The underlying principles for the GMPEs that are proposed herein are as follows:

1. Median GMPEs should be selected from published (or peer-reviewed) equations. We use a reasonable selection of such equations based on judgment , but do not attempt to include/assess all proposed models.
2. Epistemic uncertainty in median GMPEs has often been modeled by the use of alternative equations, with model weights being used to represent the relative confidence in the model alternatives, as we wish them to be reflected in the results. However, this is not necessarily the best way to model epistemic uncertainty in GMPEs (see Bommer and Scherbaum, 2008;

Atkinson, 2010). To the extent feasible, we prefer to use the alternative GMPEs and applicable data to guide the choice of a representative or "central" GMPE, and to define bounding (upper and lower) GMPEs that express uncertainty in the central GMPE.

3. It is proposed for logistical convenience that a set of 3 alternative weighted GMPEs will be used to describe the epistemic uncertainty.
4. The relative performance of the models, and a check on whether they fairly represent epistemic uncertainty, may be assessed by comparing the proposed GMPEs to each other, and to available ground-motion data as appropriate.
5. We make an initial estimate of epistemic uncertainty for each GMPE type or region, then revisit the epistemic uncertainty across regions to ensure overall logical consistency.
6. The GMPEs will be given for the reference B/C condition (Vs30=760 m/s) for input to the hazard model. Models not available for B/C will need to be converted to an equivalent model for B/C for the hazard calculations.
7. The magnitude measure for the GMPEs is moment magnitude (**M**). Thus recurrence relationships will need to be developed in terms of this magnitude scale. A variety of distance metrics are used in the GMPEs, and these may be converted to an equivalent point-source metric (hypocentral distance) in the hazard software as needed (this is software dependent, as FRISK88 uses point-source representations within areal sources, whereas other software such as EZFRISK handles the issue of distance metric implicitly).
8. Conversions in the hazard software between Repi (epicentral distance) and Rjb (Joyner-Boore distance, based on distance to surface projection of rupture plane), or between Rhypo (hypocentral distance) and Rcd (closest distance to fault rupture surface) may be made using an approximation, described in Appendix A, that accounts for average fault size (which may be regionally dependent). Other approximations could also be used.
9. To ensure reproducibility of the recommended GMPE suite in other PSHA applications and facilitate checking against various equations and datasets, tables of the final recommended GMPEs as used in the hazard calculations are posted at www.seismotoolbox.ca.

Eastern GMPEs (crustal)

We propose to use ENA GMPEs of several different types (differing classes of approaches) developed within the last 10 years, to sample the field. The proposed GMPEs are described below (in reverse chronological order of publication); we include relations that are useable over the entire magnitude/distance range of interest to the computations (**M**4.8 to 8 at distances to 500km).

PZT11: Pezeshk, Zhandieh and Tavakoli, 2011
This GMPE is based on the hybrid empirical approach developed by Campbell (2003), but uses an updated model for both the ENA parameters and the WNA reference equations. The idea is that a stochastic point-source model is used to derive adjustment factors for WNA GMPEs, based on differences in model inputs between ENA and WNA. The parameter values are simple and well motivated. Though this GMPE is very "new", it was reviewed by several of the top experts in the field and has been published in BSSA (Aug. 2011). (Note: a comprehensive update of the Campbell (2003) GMPE has not yet been done.)

The PZT11 GMPE is specified for hard rock site conditions, so must be converted to B/C. PZT11 use the Atkinson and Boore (2006) (AB06) values of amplification and kappa for ENA hard rock (~2000m/s), and the corresponding values from Boore and Joyner (1997) for WNA rock (~600m/s), in their model to derive correction factors from WNA to ENA. This follows the amplification factors used by AB06, so that we can use conversion factors from A to B/C based on AB06 to predict the corresponding B/C motions for the PZT11 model (from their hard-rock GMPE values).

The conversions from hard rock to B/C have been simplified by noting that they show little dependence on magnitude or distance, over the magnitude range from 5 to 7, and distances from about 5 to 300 km. Constant values (in log10 units) can be added to the hard rock predictions (for log10 PSA) to get equivalent predictions for B/C, as follows:

PSA:freq(Hz)	(BC-A)
0.2	0.06
0.5	0.09
1	0.11
2	0.14
3	0.14
5	0.12
10	0.03
20	-0.1
PGV	0.09
PGA*	-0.3+0.15log(Repi)

* PGA value may also be used for PSA at f≥40 Hz.

The conversions were derived by plotting the differences (in log10 units) between AB06' predictions on B/C and those on A, as functions of magnitude and distance. As noted above, the factors are insensitive to magnitude. The factors listed are for **M**=6, but would be only about 0.02 units lower for **M**=5, or 0.02 units higher for **M**=7; this is trivial given other uncertainties. The factors are also insensitive to distance, except for very high frequencies (>30Hz) and PGA; a distance-dependent factor is given for PGA (which can also be used for 40 Hz PSA).

The distance variable in PZT11 is closest distance to the fault (Rcd), which can be approximately estimated from epicentral distance using the conversion equations for ENA fault sizes (Appendix A).

AB06': Atkinson and Boore, 2006 (as revised in Atkinson and Boore, 2011)

This GMPE model is based on a stochastic finite-fault approach, which is a simulation approach that uses a seismological model, with key parameters calibrated based on ENA ground-motion data. It is one of a very small number of recent published ENA GMPEs that includes both a comprehensive model and a comprehensive comparison of the model against ENA data. Coefficients are provided for both B/C and hard-rock conditions, so we can use the B/C version directly. The equations were recently updated (Atkinson and Boore, 2011) to agree better with moderate-magnitude earthquake data, and with WNA-scaling of motions with magnitude. The updated version is referred to as AB06'.

The distance variable in AB06' is Rcd. Care should be taken in converting to Rcd from hypocentral distance as the model does not build in distance-saturation effects, but instead relies on keeping the fault a reasonable distance away (i.e. the assumption of a buried fault) to avoid this problem. Atkinson and Boore (2011) recommend using a minimum depth to the top of the rupture (Ztor) that depends on magnitude, in order to place minimum constraints on the value of Rcd that is associated with near-epicentre distances. These minimum values for Rcd should be applied following the conversion, if necessary. (e.g. Rcd is the value given by the conversion equations from Rhypo, but constrained such that Rcd(min) = Ztor = 21 – 2.5 **M ;** in other words, if the calculated value of Rcd from the Goda et al., (2009) equations exceeds (21-2.5**M**), we use (21-2.5**M**) in its place.) Note this minimum value decreases from Rcd(min)= 8.5 km at **M**5 to Rcd(min) = 2.3 km at **M**7.5.

A08': Atkinson, 2008 (as revised in Atkinson and Boore, 2011)
This GMPE is based on a referenced empirical approach, which is similar in concept to the hybrid empirical approach, but uses ENA data directly to derive adjustment factors to WNA GMPEs. It is a useful inclusion from the point of view of epistemic uncertainty as it suggests a smoother attenuation function than do model-based approaches (like AB06' and PZT11). Coefficients are provided for B/C conditions. The distance metric is closest distance to the surface projection of the rupture (Rjb), which can be estimated from epicentral distance using the equations of Goda et al. (2009). This model was recently updated by Atkinson and Boore (2011) to use modified BA08' GMPEs for WNA (see sections below) as the reference; these modifications account for recent moderate-magnitude observations in both ENA and WNA. The modified version is referred to as A08'.

SGD02S: Silva, Gregor and Daragh, 2002, Single-corner (variable stress)
This GMPE has never been formally published (except on the authors' website) but has been very widely used; it is recommended for inclusion for this reason, as an 'industry-standard' stochastic point-source model (in which stress drop decreases with magnitude to mimic WNA saturation effects). It is given for hard-rock conditions, so must be converted to B/C; the conversion factors based on AB06 can be used for this purpose, as the amplification model employed by the authors is very similar to that of AB06. The distance variable is Rjb, which can be estimated from epicentral distance using an approximation (Appendix A).

SGD02D: Silva, Gregor and Daragh, 2002, Double-corner (with saturation)
This is another variant of the SGD02 model, in which a double-corner stochastic point-source model is used in the simulations, to consider epistemic uncertainty in source. As for the SGD02S model, it needs to be converted to B/C, and the distance metric is Rjb.

Comparisons of the proposed ENA GMPE suite for B/C conditions is given in the following figures, for **M**=5, **M**=6 and **M**=7, at 1 Hz and 5 Hz. In these figures the approach described by Atkinson and Boore (2011) is used in converting Rcd to Rjb for plotting purposes (based on the top of rupture formula discussed above, where Rcd = $\mathrm{sqrt}(Rjb^2 + Ztor^2)$). ENA data within 0.5 magnitude units of the prediction line, converted to B/C conditions from hard rock, are overlain on the figures, from the database of Assatourians and Atkinson (2010) (lower half of magnitude range in black, upper half in orange). The figures indicate reasonable agreement between the models and the data, with increasing epistemic uncertainty at larger magnitudes (particularly at lower frequencies) where data are sparse. Note there is a lot of scatter in the plotted data as they cover an entire magnitude unit, and inevitably contain some variability due to different sit conditions at the recording stations (though all are nominally on “rock”). The purpose of the plot is mainly to give an indication of the data, rather than match it to the curves in any quantitative way.

It may be noted that another well-known ENA GMPE that is not among this suite is the relationship of Somerville et al. (2002). The Somerville et al equations were based on deterministic broad-band simulations, using a methodology this is applicable to larger events (**M** 6 and greater). The methodology and equations are well-founded and considered applicable. However, because the events of **M**<6 are important to hazard estimation, this equation is not used directly, to avoid possible bias for events of **M**<6. Instead, I note that the Somerville et al. (2002) equations fall within or just below the range of the equations suggested for implementation in the following (median ± one standard deviation) for events of **M**>5.75. There is a tendency for the Somerville et al. GMPEs to predict somewhat lesser motions for epicentral distances <20 km and >200 km, in comparison to those in this suite. This suggests that the proposed suite of equations may be somewhat conservative for close distances.

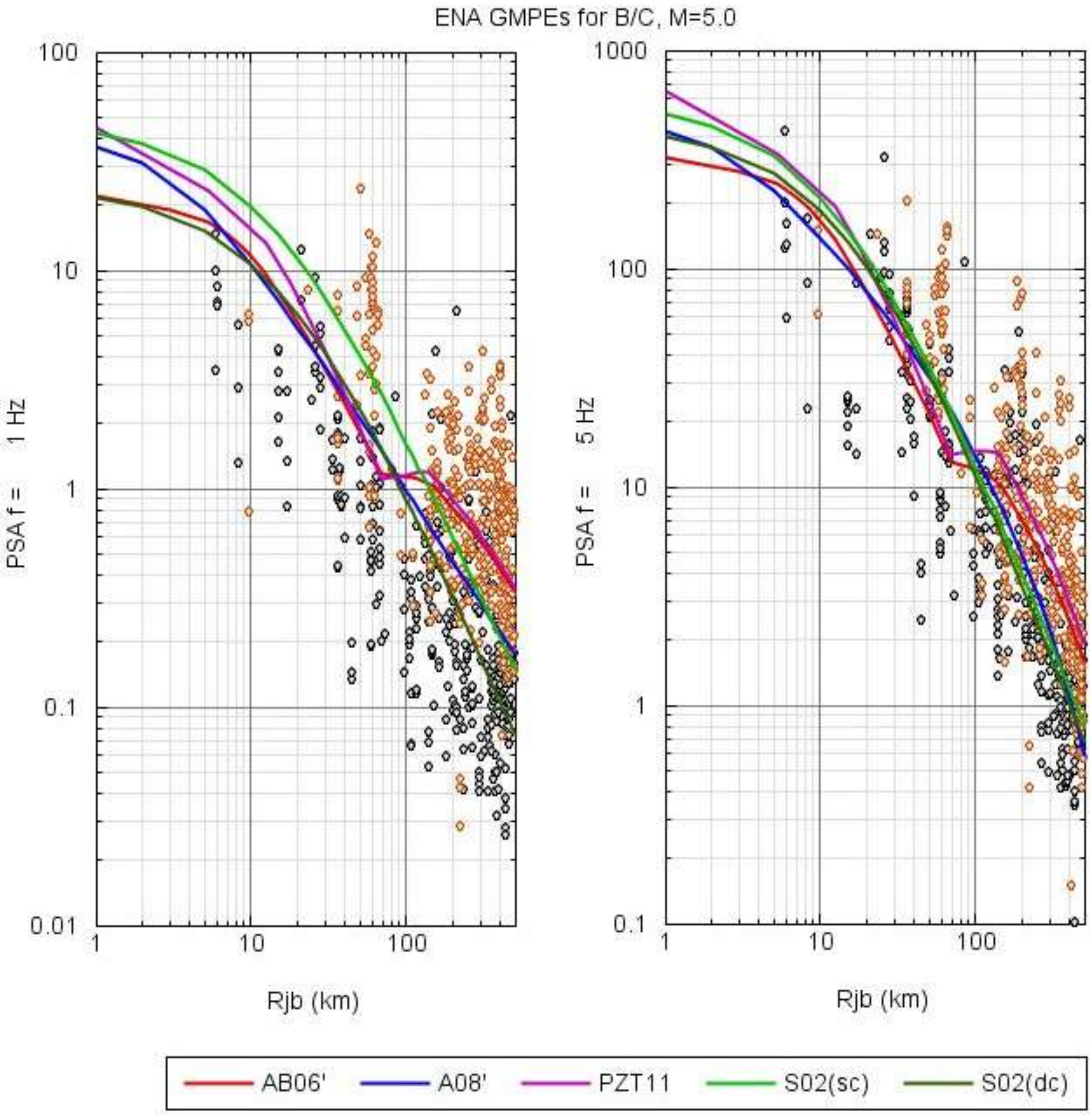

Figure note: ***M****4.5-5.0 data in black,* ***M****5.0-5.5 data in orange. All data converted to B/C.*

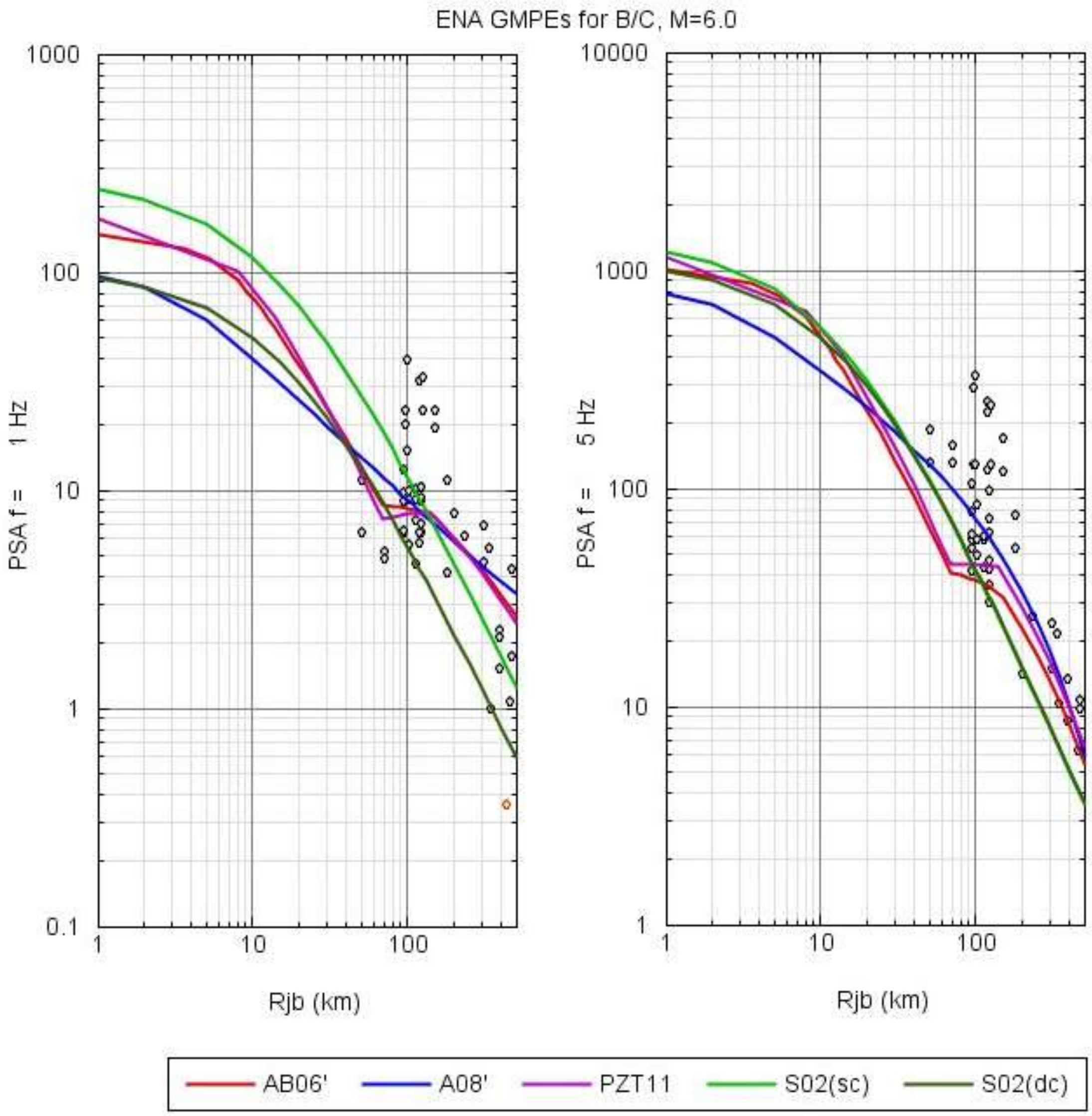

*Figure note: **M**6 data are from Saguenay (**M**5.9) only (converted to B/C site conditions).*

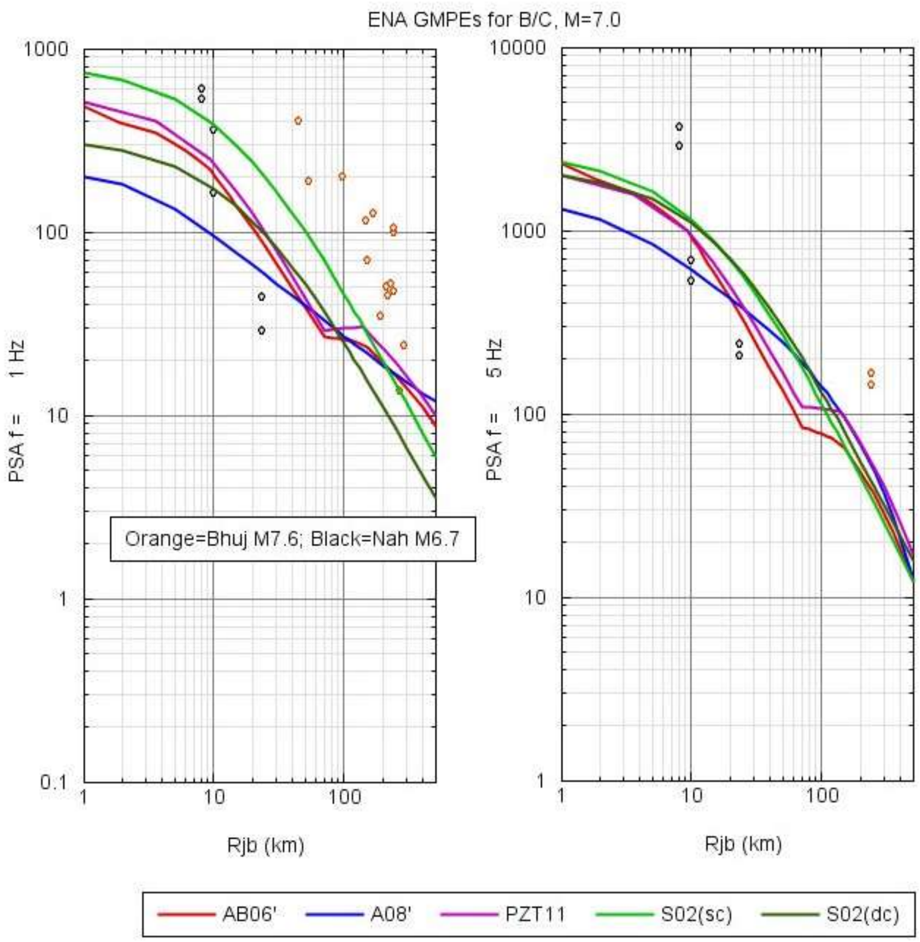

Implementation of ENA GMPEs

We implement the five ENA GMPEs by defining a suite of 3 relationships that express the geometric mean (i.e. median) ground motions of the five alternative estimates for each magnitude-distance-frequency, as well as the median ± one standard deviation. To obtain smooth prediction curves, we calculate the mean of the log values for the 5 GMPEs at **M**=4.5, 5.0, 5.5,…..8.0, evaluated at epicentral distances of 1, 2, 5, 10, 20, 50, 100, 200 and 500 km (for a fixed focal depth of 10 km), along with its standard deviation. (Note: the conversion from the distance metric of each GMPE to epicentral distance is made as described in Appendix A, assuming ENA fault dimensions.) We smooth the standard deviation using a triangular 3-point weighted smoothing. For example, the smoothed standard deviation at 2 km is obtained as 0.25*(std.dev. at 1 km) + 0.5*(std.dev. at 2km) + 0.25*(std.dev. at 5km); first and last distance points use equal 2-point smoothing with nearest neighbour. The smoothing avoids "pinching" of the upper and lower representative relations at certain distances where the five estimates fortuitously happen to lie close together. The sets of GMPEs are implemented in table format in the hazard software, so that no "fitting" to the values is required (the table in log PSA vs. log distance is interpolated to find the value corresponding to any **M**, distance and frequency).

The figures below provide an illustration of the mean-value GMPE from the 5 candidate relations, along with the corresponding plus and minus standard-deviation GMPEs. The Atkinson and Boore (1995) equations, used in the NBCC2005 maps, are shown for reference (for B/C). The epistemic uncertainty obtained using this procedure varies with magnitude, distance and frequency; averaged over all magnitudes, distances and frequencies, the upper and lower curves differ from the mean curve by 0.17 log(10) units (factor of 1.5). This provides an initial estimate of epistemic uncertainty in the eastern crustal GMPEs, which we revisit later in comparison to the GMPEs for other regions.

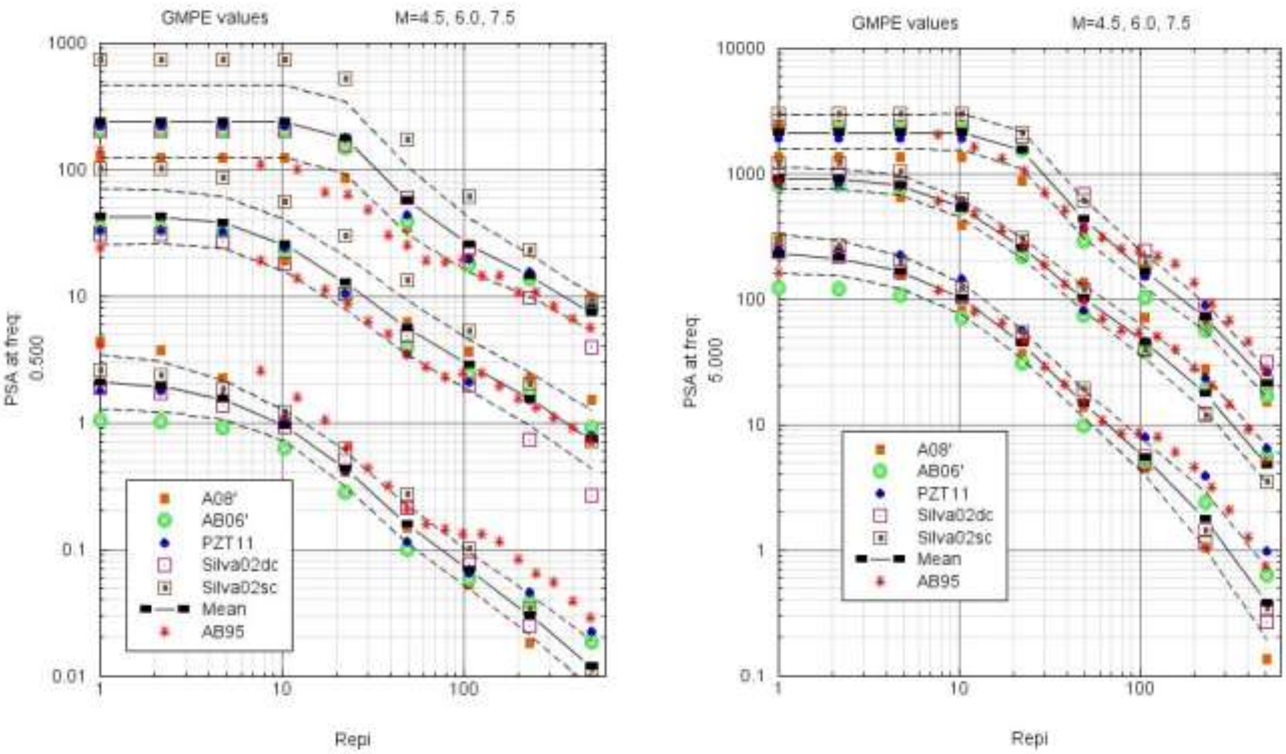

Figure: PSA values at 0.5Hz, 5Hz,(M=4.5, 6.0, 7.5) for 5 ENA GMPEs versus epicentral distance, along with geomean values (black squares), and relations giving mean±standard deviation. Red asterisks show AB95 equations used in 2005 NBCC maps.

Western crustal GMPEs

A common assumption made for crustal earthquakes in B.C. is that their ground motions will be well represented by GMPEs for other active tectonic regions, such as California. This may be so, if differences in predominant site conditions are accounted for – in particular the fact that much of B.C. has been glaciated while California has not. A paper by Atkinson (2005) looked at this issue and concluded that, overall, crustal earthquakes in B.C. might be modeled using typical WNA crustal equations (though they appear to over-estimate motions in B.C. at the small-to-moderate magnitudes available), and gave factors to convert between California and B.C. rock conditions. A B.C. Hydro study in 2009-2010 supported this general conclusion. Since we are using B/C as a reference condition, no conversions for different rock conditions will be required – but it should be kept in mind that any comparisons of the GMPEs with B.C. data should convert the hard-rock data (Vs30~1500 m/s) to B/C (Vs30=760 m/s).

The suite of GMPEs currently favoured for crustal events in active tectonic regimes is the PEER-NGA equations (Power et al., 2008 and the references therein), due to its extensive and high-quality database (especially at the near-source distances important to hazard) from diverse active regions worldwide. A few challenges arise in using these equations, some logistical and some scientific:

(1) many of them involve a level of detail in the parameter specifications that go beyond what is available/reasonable for western Canada, leaving many parameters to be defined by default “guesses”;
(2) it is known that these GMPEs tend to over-estimate motions from moderate events (Atkinson and Morrison, 2009; Chiou et al., 2010; Bommer et al. 2007; Cotton et al., 2008; Atkinson and Boore, 2011), but only two of the equations (BA08 and Chiou and Youngs) have published corrections for this effect – which might be important in low-to-moderate seismicity regions of B.C.;
(3) The GMPEs agree “too closely” with each other, and thus probably don’t actually the true convey epistemic uncertainty in median values (Abrahamson et al., 2008; Atkinson, 2010).

To overcome these challenges, we define a 3-equation suite that is based loosely on the PEER-NGA equations. We use the modified (for moderate-magnitude) BA08’ equations for “unspecified” fault mechanism as a reference suite (they are the simplest, and do not require specification of unknown variables), and use the other PEER NGA equations to estimate the uncertainty on these equations. The following figure provides a guide to bounds on the median equation to reflect epistemic uncertainty. In the figure, the alternative NGA equations of Boore and Atkinson, Abrahamson and Silva, Campbell and Bozorgnia, and Chiou and Youngs are plotted for PSA at 1 Hz and 5 Hz, for **M**=6.5 (top) and **M**=7.5 (lower), all for B/C conditions. To put the equations in an empirical perspective, the NGA data (also converted to B/C, as in Boore and Atkinson, 2008) are plotted in magnitude bins 0.5 units in width, in distance bins 0.4 log units in width. For the central magnitude value (e.g. 6.5 or 7.5), the mean and standard deviation of the amplitudes within the bin is plotted. For magnitude bins 0.25 units less or greater than the central value, the means are plotted (without standard deviations, to avoid clutter); note that the magnitude bins have a 50% overlap. As noted in Abrahamson et al. (2008), the NGA equations are all fairly similar, and all are reasonably (though not perfectly) constrained by the data. A subjective judgement based on the figure is that the epistemic uncertainty in median equations can be reasonably modeled by adding and subtracting 0.1 to 0.15 units log(10) (25% to 40%) from the BA08’ equations, to give upper and lower bound equations, respectively. (Reasonable relative weights would be 0.5 for the middle curve, and 0.25 for the lower and upper curves.) This would encompass the NGA equations and most of the data constraints fairly well. It should be noted that use of this approach does not imply a preference for the BA08’ equations – all of the NGA equations have the same degree of validity. Rather, it is a convenience of application that the NGA results may be encapsulated by taking BA08’, the simplest of the models, as representative, and using factors about it to bracket the family of GMPEs. The sensitivity of the hazard calculations to the model spread and its weights should be tested in order to assess whether a reasonable level of epistemic uncertainty has been achieved with the proposed approach. Epistemic uncertainty is revisited in a later section.

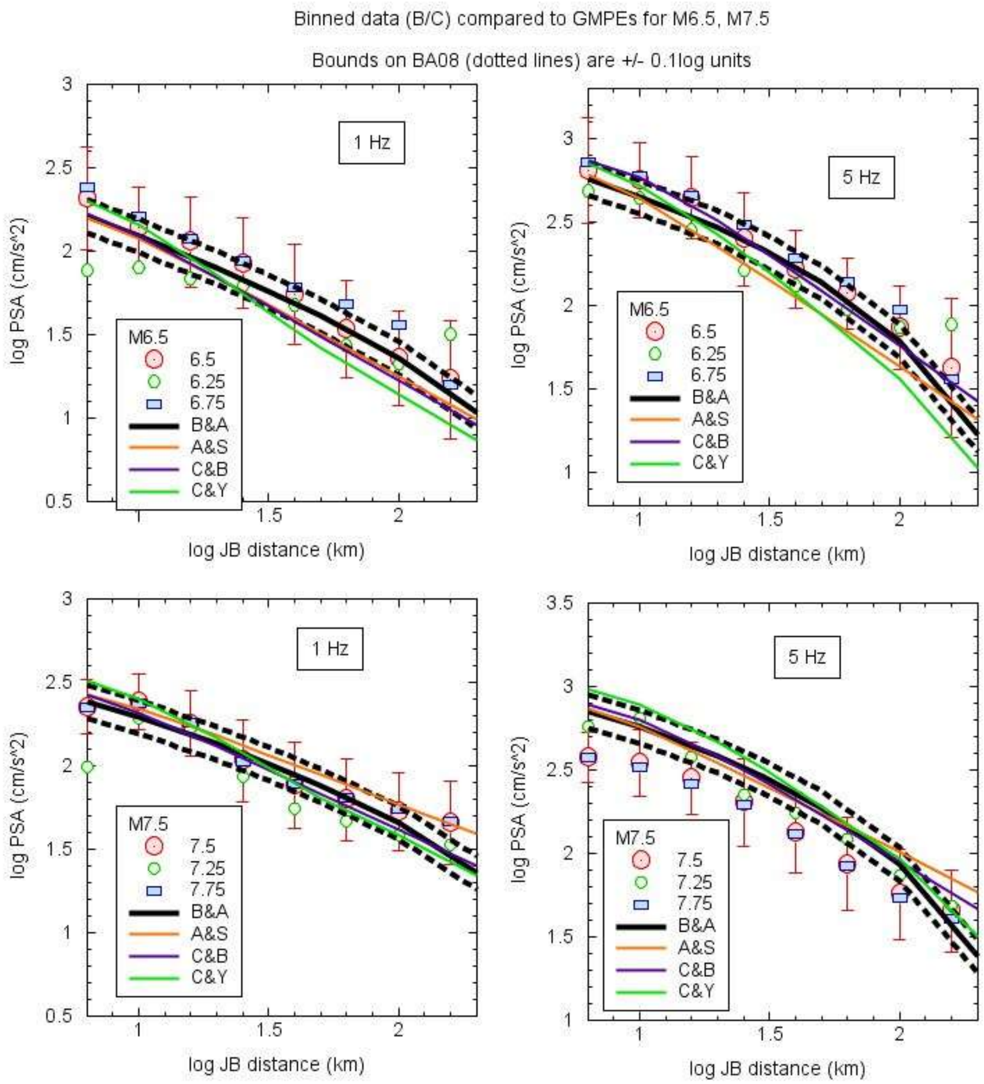

Figure notes: Solid lines show NGA equations. Dashed black lines are BA08 ± 0.1 log units. Note that for these magnitudes (M>6), BA08=BA08'. Symbols show mean data amplitudes for 0.5 unit magnitude bins; error bars show standard deviation for central magnitude bin.

Offshore crustal events

A paper by Atkinson (2005) examined differences in ground motion source and attenuation properties for different classes of events in B.C., and found that: (i) those along the west coast of Vancouver Island (just offshore) showed similar apparent source properties to crustal events in B.C., but steeper attenuation; and (ii) the events far off-shore (oceanic crust) have much lower apparent source amplitudes than crustal events, but a similar apparent attenuation. We can treat these characteristics in an approximate manner in the hazard analysis, as these events are not major hazard sources.

For the events along the west coast of Vancouver Island – within 50 km of the Island – we can use the crustal GMPEs. The use of crustal GMPEs will be conservative as the actual attenuation for these events may be somewhat steeper. For offshore events (>50 km offshore), we can follow the recommendation of Atkinson (2005) that the motions can be approximated by using crustal GMPEs, but with a reduction of 0.5 moment magnitude units. Thus if the actual moment magnitude of an offshore event is 7.0, we predict its ground motions using **M**=6.5. This is consistent with the observation (Ristau et al., 2003, 2005) that **M** = ML + 0.7 for offshore events. It is important to note that magnitude ML values must be converted to **M** before deriving the magnitude-recurrence parameters, if this approach is to be used (i.e. catalogue magnitudes ML should be converted to **M** using the Ristau et al. formula).

This approach may be illustrated using data from the Sept. 2011 **M**6.3 earthquake that occurred offshore from Vancouver Island. The Feb. 2012 **M**5.6 offshore event may also be examined. The figure below plots horizontal-component response spectra (on rock sites) in comparison to the BA08' equations (B/C boundary) for **M** = 5.5 and 6.5. The suggested approximation appears to be reasonable in relation to these limited data, although interestingly the motions from the **M**5.6 event were nearly as strong as those from the **M**6.3 event.

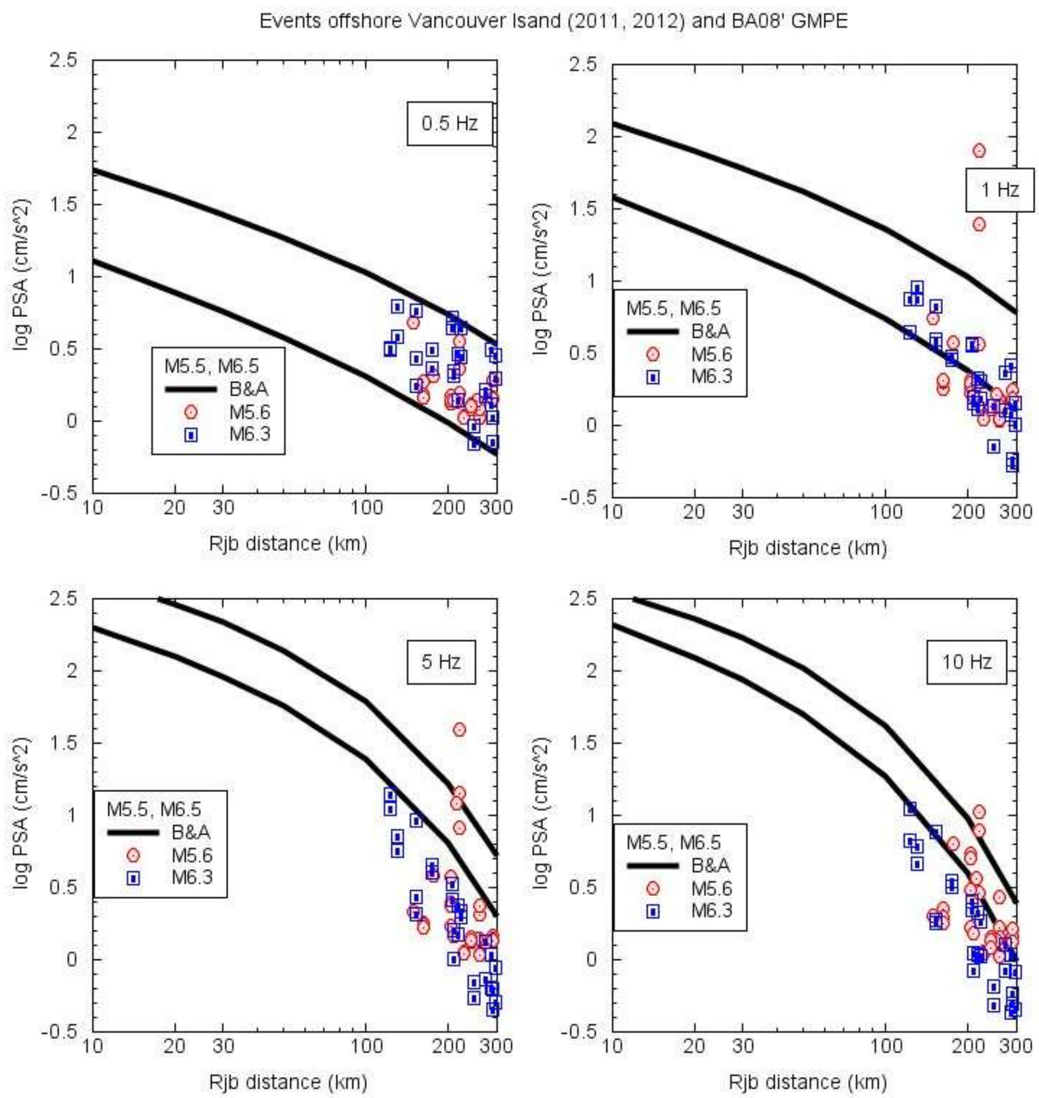

*Figure: Horizontal-component response spectra from 2011 **M**6.3 and 2012 **M**5.6 offshore events (west of Vancouver Island), compared to BA08' equations for **M**=5.5 and M=6.5.*

Western in-slab GMPEs

Global GMPEs for subduction regions are needed to characterize in-slab and interface ground motions in B.C. For in-slab events, the Atkinson and Boore (2003) (AB03) GMPE for in-slab events is still an appropriate model, as it is heavily influenced by the Nisqually earthquake data (and provides a good fit to those data); the "rock" equations of AB03 are for NEHRP A/B sites, while equations are also given for C conditions. It is proposed to use the average of the rock and C values (geometric mean) as representative of B/C boundary site conditions. The AB03 equations have a specific term for "Cascadia" site characteristics to distinguish them from other regions, in particular Japan; Japan tends to exhibit greater high-frequency site amplification, even for the same NEHRP soil type, due to the prevalence of shallow soil sites (Atkinson and Casey, 2003). The Zhao et al. (2006) in-slab GMPE for Japan is also an appropriate choice (despite the differences in site conditions), as the basic slab characteristics (focal depths, magnitude/distance ranges utilized) for the Japanese dataset are similar to those for Cascadia; for the Z06 GMPE, the site class SC I (Vs30>600 m/s) is generally suitable as an estimate for B/C conditions. More recently, the Goda and Atkinson (2009) GMPEs for Japan provide equations (for "deep" events, >30km depth) that could also be considered for in-slab predictions (similar depth range as in Cascadia). The GA09 equations extend and update the Kanno et al. (2006) equations for Japan, and use Vs30 as an explanatory variable (this is an advantage relative to Z06 or AB03). However, the GA09 equations do not explicitly distinguish between in-slab and subduction events (the distinction is implicit, using depth as a proxy for event-type classification). The following figure, from Atkinson and Goda (2010), compares the AB03, Z06 and GA09 GMPEs with the classic Youngs et al. (1997) GMPE used in the 2005 hazard maps. An additional figure compares the in-slab equations for **M**=7. Note that the attenuation shown in the Y97 relations is shallow, as it was pegged to match that for interface events (due to lack of in-slab data at the time the equations were developed). New in-slab GMPEs have been developed by Abrahamson et al. (2012), and are considered in Appendix B.

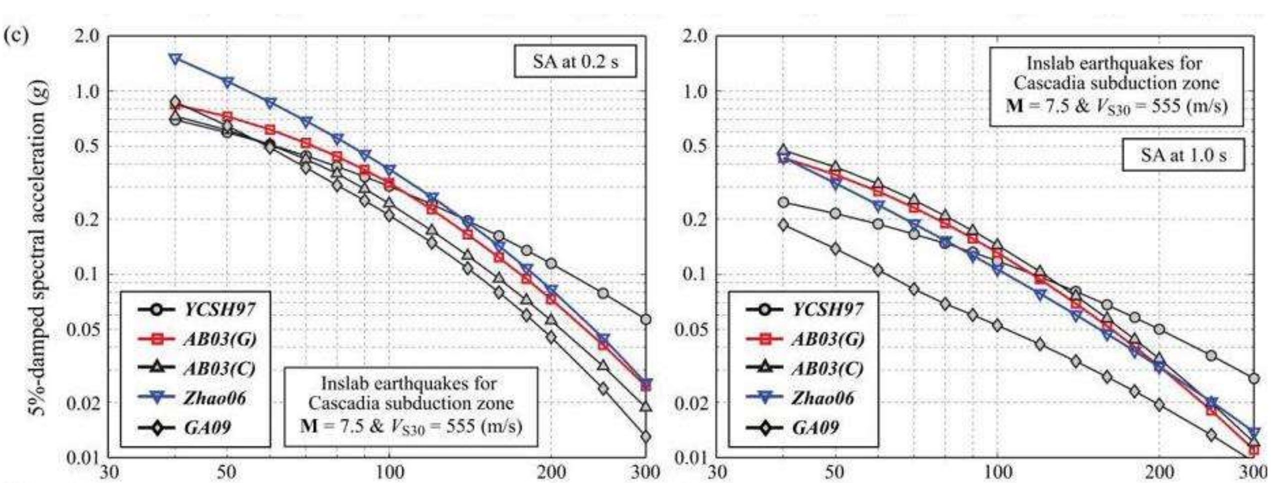

Figure notes: Comparison of in-slab GMPEs (from Atkinson and Goda, 2010). Note the Youngs et al. 1997 equation (YCSH97) has a different slope because in-slab attenuation was not considered at the time of that study (early 1990s).

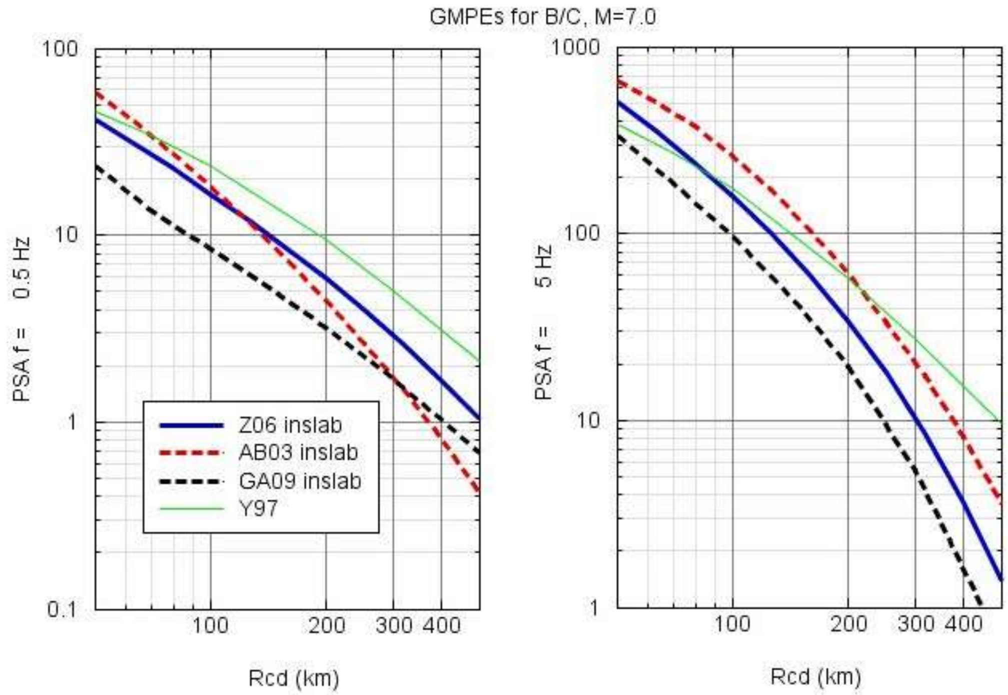

Figure: Comparison of in-slab GMPEs for M7 B/C): AB03 (Cascadia), Zhao06 and GA09. Y97(in-slab) shown for reference.

Modifications of GMPEs for inslab (and interface) to account for Cascadia site conditions

Most of the recent GMPEs for inslab and interface events are dominated by Japanese data, because they are so plentiful (e.g. Zhao et al., Goda and Atkinson). It is known that shallow site conditions in Japan result in amplifications of high frequencies relative to low frequencies, that are not captured by the use of Vs30 or site class; for example, a NEHRP C site in Japan is typically a shallow soil site overlying rock. Detailed analysis of the Tohoku motions (Ghofrani and Atkinson, 2011, 2012) have shown that these amplifications are commonly a factor of 5 or more at frequencies of 5 to 10 Hz. By contrast, site conditions in the Cascadia region are quite different, with more amplification at longer periods, and less at high frequencies. It would be reasonable and prudent to make an adjustment in the use of GMPEs from Japan to account for this well-known factor.

A simple and transparent adjustment can be made based on the study by Atkinson and Casey (2003), which compared motions from two **M**6.8 in-slab earthquakes, the Nisqually and Geiyo events, and used regression analysis to show that there is a frequency-dependent difference between the two that can be attributed to different typical site conditions, within the same site class. An important point to recall from the Atkinson and Casey study is that they also showed that the attenuation rates for in-slab events are similar for Japan and Cascadia – thus the Japan-based GMPEs are appropriate if suitable adjustments for site effects can be made. These points are illustrated in the figure below, extracted from Atkinson and Casey.

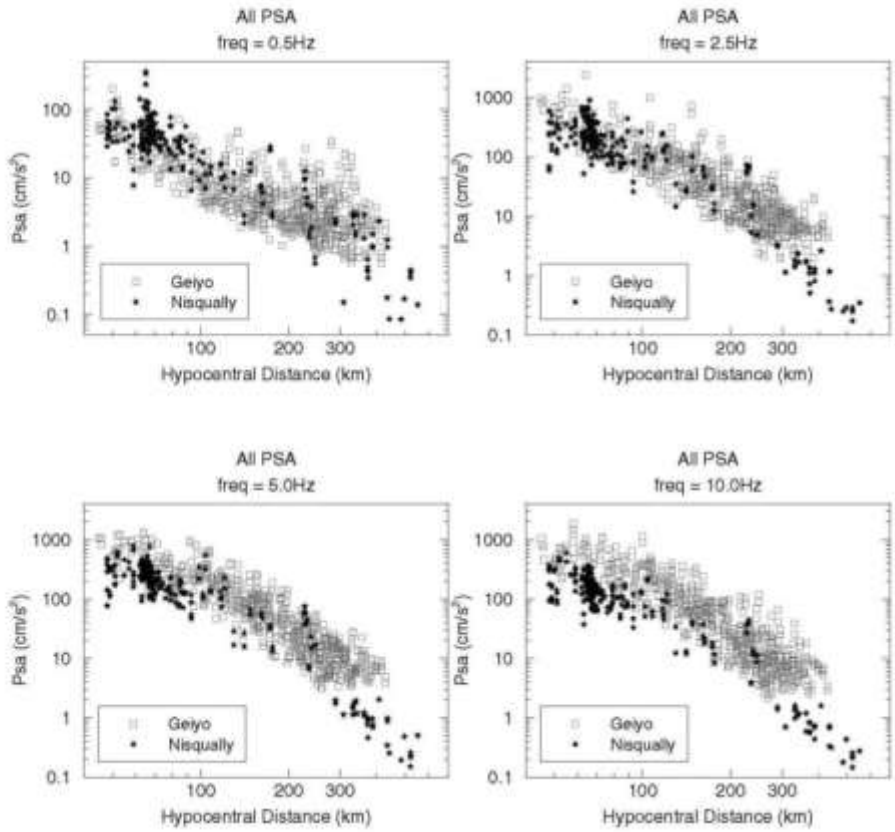

Figure 2. Response spectral amplitudes versus hypocentral distance for the Geiyo (gray boxes) and Nisqually (black stars) events at frequencies of 0.5, 2.5, 5.0, and 10.0 Hz (all data).

Figure: Response spectral amplitudes versus distance for ***M****6.8 Nisqually (Cascadia) and Geiyo (Japan) in-slab events. From Atkinson and Casey (2003).*

Atkinson and Casey showed that the discrepancies between the Geiyo and Nisqually motions disappear if we remove the expected regional site effects, computed from quarter-wavelength calculations from generic regional profiles for a given site class, and from the work of Frankel et al. for the Nisqually event (factors in Table 2 of their paper). Thus to “convert” a Japan GMPE for Class C to an appropriate equivalent for Cascadia Class C, we would multiply the predicted motions by a factor that is the ratio of (Cascadia NEHRP C/Japan NEHRP C).

An alternative approach to regional correction factors is that determined by regression analysis by Atkinson and Boore (2003). Their Table 3 shows regional factors for Japan and Cascadia, which can be used to compute the ratio Cascadia/Japan as in Atkinson and Casey. The difference is that the Atkinson and Boore factors were based on empirical data results (for Cascadia and Japan relative to the global average GMPEs) rather than computations for idealized soil profiles. The table below compares the factors suggested for the ratio Cascadia/Japan by these two alternative approaches. It is proposed to use the average of the two results, shown as “Recommended” in the table (both multiplicative and log10 factors shown). Linear interpolation in log-log space can be used for intermediate frequencies. Note that the factor is greater than unity for f<2.5 Hz, and less than unity for f>2.5 Hz.

Table:		Cascadia/Japan site factors:	
Freq.(Hz)	Atkinson&Casey	Atkinson&Boore	Recommended Cascadia Multiplicative Factor (log)
0.1			1 (0.000 log units)
0.2			1.10 (0.04 log units)
0.33		1.23	1.20 (0.079 log units)
0.5	1.47	1.55	1.51 (0.179)
1	1.08	1.00	1.04 (0.017)
2.5	1.16	0.83	1.00 (0.000)
3.33			0.81 (-0.091)
5	0.71	0.50	0.60 (-0.222)
10	0.53	0.35	0.44 (-0.357)
25		0.35	0.44 (-0.357)
PGA		0.45	0.50 (-0.301)
PGV			1.00 (0.000)

The site correction factors should be applied to both in-slab and interface GMPEs that are based predominantly on Japanese data – these would include Zhao et al., 2006 (in-slab and interface) and Goda and Atkinson (2009) (in-slab and interface). Note that the AB03 GMPEs for in-slab events already include a Cascadia factor (so no further adjustments needed). (It may also be mentioned that the next version of NGA-West equations, NGA-W2, will include regional adjustments for site conditions.)

The figure below shows the 3 in-slab GMPEs discussed above, for **M**=7.0, after adjusting the GA09 and Z06 equations for the factors shown in the table above. (Note: conversions to Repi for this plot are made using the inslab approximation suggested in the Appendix.) The BA08' GMPE for crustal events is shown for reference. For the AB03 equations, the Cascadia version of the GMPE, as given in AB03, is used. Interestingly, these 3 equations are now all very similar at high frequencies (10 Hz, PGA) – the adjustment for regional site condition has brought them into close agreement. At low frequencies, the GA09 GMPE is significantly lower than Z06 and AB03. This may reflect that the GA09 GMPE did not completely separate the regressions for inslab and interface events – rather, a depth term was included to adjust for amplitude level differences between the event types, and the attenuation rate differed for shallow (<30 km) versus deep (>30 km) events. This approach has some advantages in regression stability in that the entire database is utilized to control features such as amplitude level, but may be disadvantageous in the accuracy of quantifying differences between event types. As a suspected result of this approach, the GA09 GMPEs are lower than others for inslab events, and higher than others for interface events. We do not explicitly use the GA09 GMPEs for this reason.

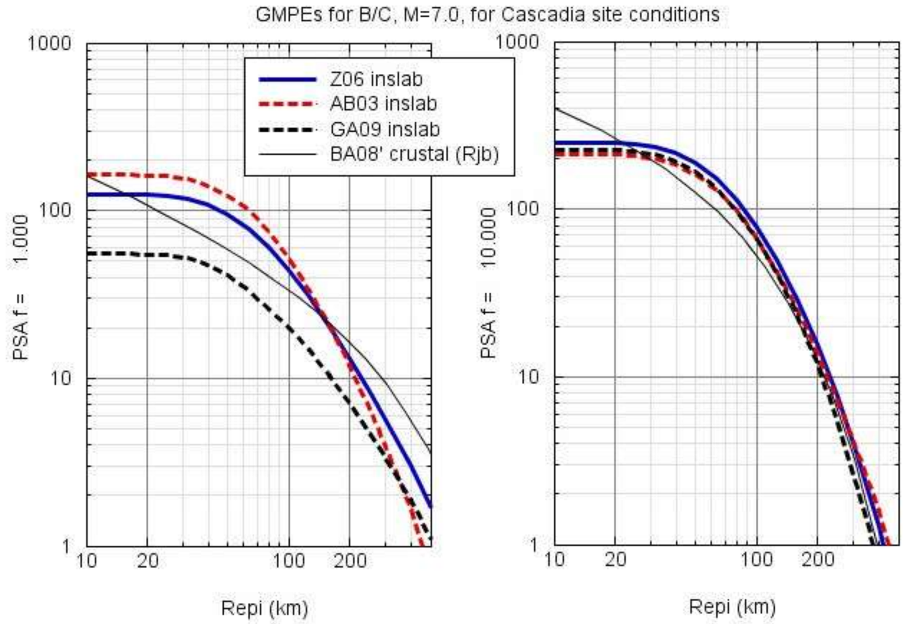

*Figure – Comparison of 3 alternative inslab GMPEs for **M**=7 in Cascadia, for B/C site conditions (after correcting Japan equations for Cascadia site conditions).*

The similarity of Z06 and AB03 after site corrections raises the possibility that perhaps the inslab GMPEs would be best represented by selecting one of these two models - the Z06 GMPEs due to its superior database - and using it as a representative GMPE (after adjustment for Cascadia site condition). The other equations may be used to guide the choice of an epistemic uncertainty band about it. Scanning through comparisons of plots such as that above, for different magnitudes and frequencies (see plots in Appendix C), this would work well EXCEPT for **M**>7.5, for which the Z06 GMPEs are significantly higher at 5 to 20 Hz than AB03 or GA09 (and also appear high at near distances compared to crustal GMPEs such as BA08'). Because the maximum magnitude for the in-slab sources is ≤7.5 in our application, this is not an issue. (Note: if required, the Z06 GMPE could be forced to saturate for **M**>7.5 by assigning the Z06 motions calculated for **M**=7.75 to the magnitude of **M**=8 in the GMPE tables.) We revisit the in-slab equations, their comparison with data, and the question of how to express epistemic uncertainty in the inslab GMPEs later (see also Appendix B).

Western interface GMPEs

For interface events, both empirical and simulation-based GMPEs may be used to model the expected Cascadia mega-thrust motions. Amongst empirical GMPEs, those of Zhao et al. (2006) for subduction events are suggested. Gregor et al. (2002) and Atkinson and Macias (2009) both provide a simulation-based model derived from stochastic finite-fault simulations. The methodology used by Gregor et al. and Atkinson and Macias is similar, but the Atkinson and Macias (2009) GMPE is calibrated based on larger, more recent interface events (the **M**8.3 Tokachi-Oki event), and is developed for the reference condition of B/C boundary (the Gregor et al. equations are given for "rock" or "soil", but the specified rock Vs30 is only 363m/s, which is significantly softer than B/C). The use of simulations is important for Cascadia subduction events due to the lack of recorded data for the expected type of event (**M**>8.5 with B.C. attenuation).

Another possible choice that is sometimes suggested for interface GMPEs is to include a crustal model from active regions (e.g. BA08). It is often argued that shallow crustal events and shallow interface events within a subduction region appear to have similar source parameters and attenuation characteristics; this is evidenced by the similarity of typical GMPEs developed for interface events, in comparison to GMPEs developed for crustal events, for moderate events, over most period ranges (e.g. Si and Midoridawa, 1999; Zhao et al., 2006). By contrast, deeper in-slab events have significantly greater short-period amplitudes at near-source distances, and steeper attenuation rates (Atkinson and Boore, 2003; Kanno et al., 2006; Zhao et al., 2006; Goda and Atkinson, 2009).

These points are considered in the figure below, which compares the attenuation characteristics of crustal, inslab and interface events for an event of **M**=7.5, based on recent GMPEs. In order to provide a consistent set of equations that illustrates the differences between event types, we plot the Zhao et al. (2006) equations; Zhao et al. compiled a large database (from Japan and other active regions) and then used a single regression analysis to distinguish the source levels and attenuation from each of the event types. An alternative to the Zhao et al. (2006) equation is shown for comparison, for each event type. Note that differences between investigators in amplitude levels can be significant (e.g. compare Boore and Atkinson, 2008 to Zhao et al., 2006, for crustal events), due to differences in the datasets used and the regression methodology. However, some overall trends may be noted. Specifically, the in-slab events have higher amplitudes at fault distances < 100 km than other event types, but attenuate more rapidly. Crustal and interface events appear to have similar amplitudes and attenuation at low frequencies, but the interface amplitudes appear to be larger at high frequencies. Finally, note that not all of the plotted GMPEs represent the same site condition, due to the regional differences in typical site profiles within the same site class noted in the previous section.

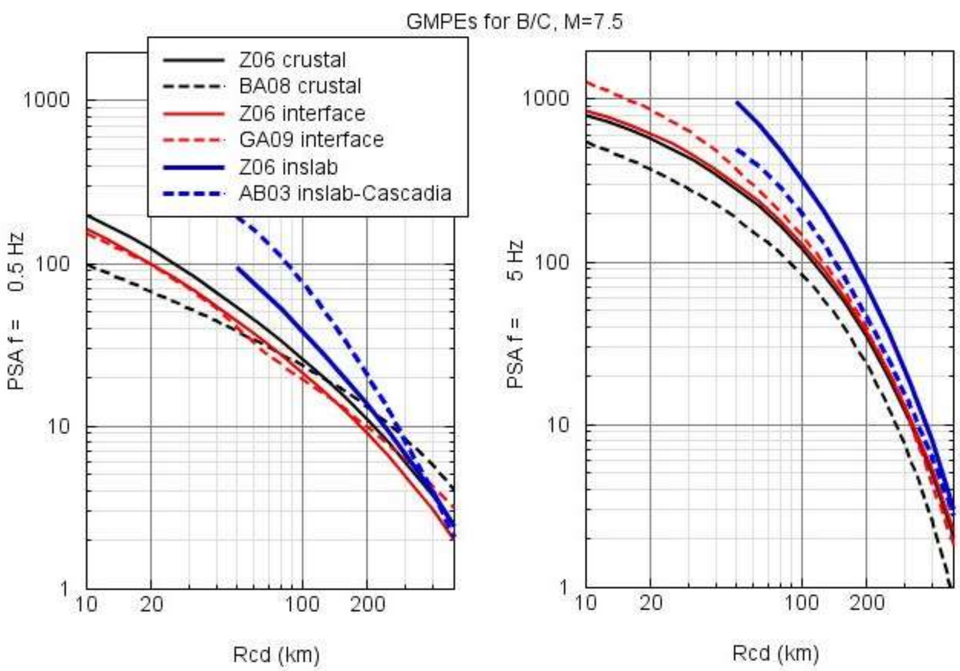

*Figure – Comparison of GMPEs for PSA (5% damped horizontal, Vs30~760m/s) versus closest-distance to fault, for **M**=7.5 events in subduction environments. Zhao et al. , 2006 (Z06) equations are developed separately for crustal (h=10 km), interface (h=20 km) and in-slab (h=50 km) events, at* *typical focal depths. An alternative equations from another study is shown for each case (AB03=Atkinson and Boore, 2003, in-slab; BA08=Boore and Atkinson, 2008, crustal; GA09=Goda and Atkinson, 2009, shallow events). The differences in the in-slab equations between AB03 and Z06 are primarily due to the inclusion of adjustment factors in AB03 for Cascadia site conditions. Relative to Japan, these factors increase low-frequency amplitudes (by 39% at 0.5Hz) and decrease high-frequency amplitudes (by 33% at 5Hz).*

Another factor to consider in selecting GMPEs for great interface earthquakes in Cascadia is new information from the 2011 **M**9 Tohoku earthquake. This is the type of event, and approximate magnitude, expected for future great earthquakes on the Cascadia subduction zone. The motions from Tohoku were very large, especially at high frequencies. This was partly due to pronounced site response effects (Ghofrani et al., 2012). The figure below compares several candidate GMPEs to the preliminary regression model from the **M**9 Tohoku data (from Ghofrani et al., 2011, SSA poster), all for a reference site condition of Vs30=760 m/s. It should be kept in mind that the Tohoku data from distances >150 km are all from back-arc sites, which is why the attenuation for Tohoku at larger distances is quite steep. In Cascadia, a gentler attenuation is expected to apply for cities in southwestern B.C. It is noted that the Tohoku motions are large relative to those expected from typical crustal GMPEs (e.g. BA08). For this reason, and in light of the ambiguity noted above as to whether crustal and interface GMPEs are indeed comparable, it is suggested that crustal GMPEs not be included in the interface suite.

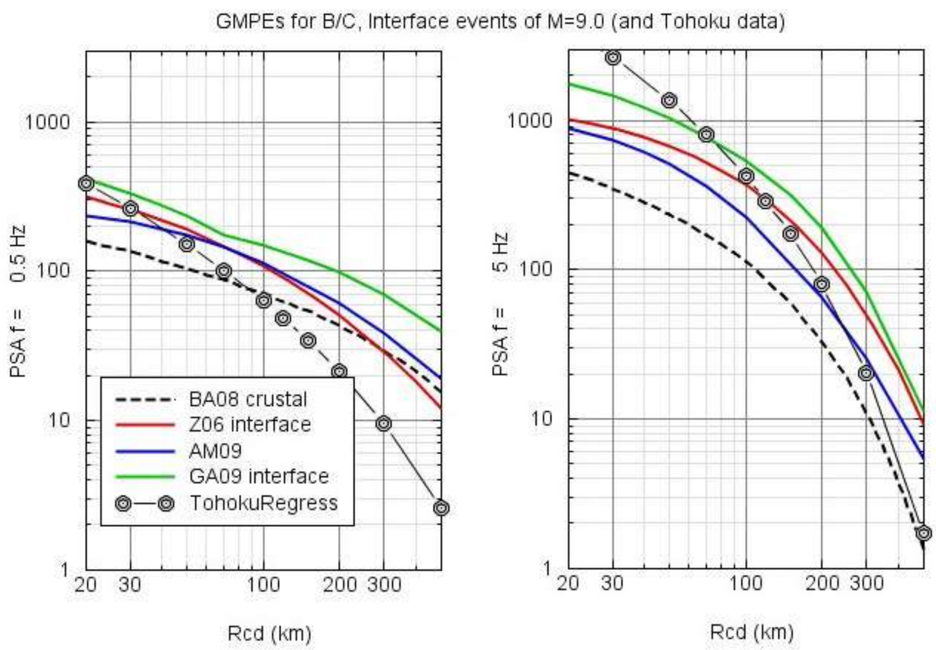

*Figure – GMPEs shown for 0.5Hz and 5Hz for **M**=9, in comparison to a preliminary regression line for the **M**9 Tohoku PSA data, all for Vs30=760m/s. Note Tohoku data at R>150 km are mostly back-arc data, and therefore attenuate quite steeply. BA08 (Boore and Atkinson, 2008) is a crustal GMPE, while others are for interface events. Z06 (Zhao et al. 2006) and GA09 (Goda and Atkinson, 2009) are empirical GMPEs while AM09 (Atkinson and Macias, 2009) is based on simulations for Cascadia, calibrated using **M**8.3 Tokachi-Oki, Japan ground-motion records.*

The AM09 equation is suggested as a backbone model because it is specific to Cascadia, but calibrated using the **M**8.3 Tokachi-Oki, Japan ground-motion records, and given for B/C conditions. The Z06 interface model (Zhao et al., 2006) is a robust empirical model. Note that all three of the models plotted above tend to predict significantly larger amplitudes than WUS crustal models, for the magnitude range 8 to 9 (typical factor ~2 for the average of the three suggested models) – this is because these models do not feature the heavy magnitude saturation seen in the PEER-NGA crustal models.

We can apply the same regional site correction factors as outlined for inslab events to interface GMPEs. The AM09 interface GMPE is developed specifically for Cascadia (B/C), so no adjustment is needed. The GA09 interface and Z06 interface GMPEs are adjusted as for the inslab versions. The figure below shows the predicted motions after adjustments, for B/C, for a **M**9 Cascadia event. The BA08' GMPE for crustal events is shown for reference. Note that the GA09 GMPE is now the highest of the suite, instead of the lowest (whereas for inslab events it was the lowest).

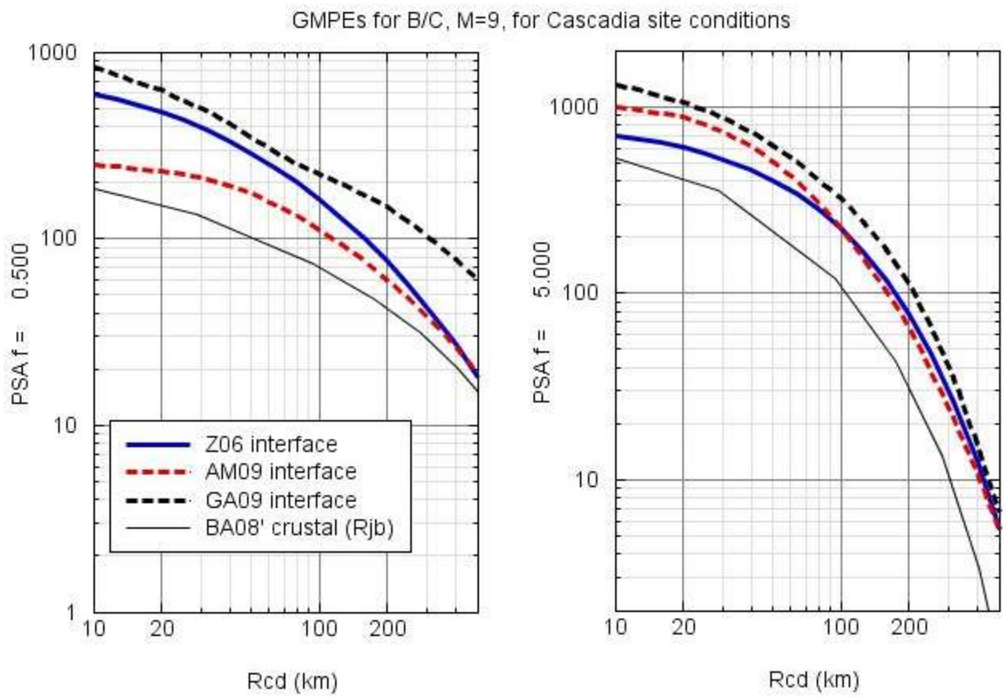

*Figure – Alternative interface GMPEs for **M**=9 B/C, after adjustment for regional site conditions. BA08' for crustal shown for reference.*

Epistemic Uncertainty in GMPEs

A primary source of epistemic uncertainty in PSHA is the GMPE uncertainty. In this section we revisit epistemic uncertainty in GMPEs, so that we can put all the proposed GMPEs and their uncertainties in a consistent context. We start with the epistemic uncertainty for crustal GMPEs in the west, for which the GMPEs are best constrained by data. We need to ensure we have enough epistemic uncertainty built in; the resulting uncertainty (median, mean, 84^{th}%) in hazard calculations will be sensitive to this choice.

I work from the premise that the "blind use" of multiple GMPEs is not necessarily the best way to express epistemic uncertainty in ground motions over all magnitudes and distances, although this is common practice. I make and inspect more plots of the proposed alternative GMPEs for a range of magnitudes, which are included in Appendix C. **Suggested preliminary weights for all of the 3-GMPE suites described below are 0.5 (med), 0.25(low), 0.25(high); adjustments are made later based on the re-evaluations shown in Appendix B.**

Western crustal GMPE uncertainty

Looking carefully at GMPE plots (western crustal events) in both log and linear scale, for the **M**=6.5 to 7.5 range, it appears that uncertainty in the median, considering the alternative GMPEs and the data that constrain them, is of the order of 0.15 log units (factor of 1.4). This also takes some account of the fact that we are transporting a global GMPE to B.C. Furthermore, it appears that the uncertainty should grow with distance, based on the spread in the PEER-NGA equations; this is also appropriate given that the NGA equations combined data from different regions, having somewhat different attenuation rates. The following log factor (delta) is recommended to add/subtract from BA08' to express epistemic uncertainty. This revised uncertainty is shown in the example plot below (others shown in Appendix C).

Delta (crustal) = min (0.10+0.0007 Rjb, 0.3) (log10 units)

Delta is "capped" at 0.3 log units to prevent large growth at greater distances. Note that the total uncertainty from low to high GMPE is about a factor of 2 for the western crustal events. This should be considered a minimum uncertainty for other event types, because the western crustal GMPEs are the most-widely studied, and best-constrained by data.

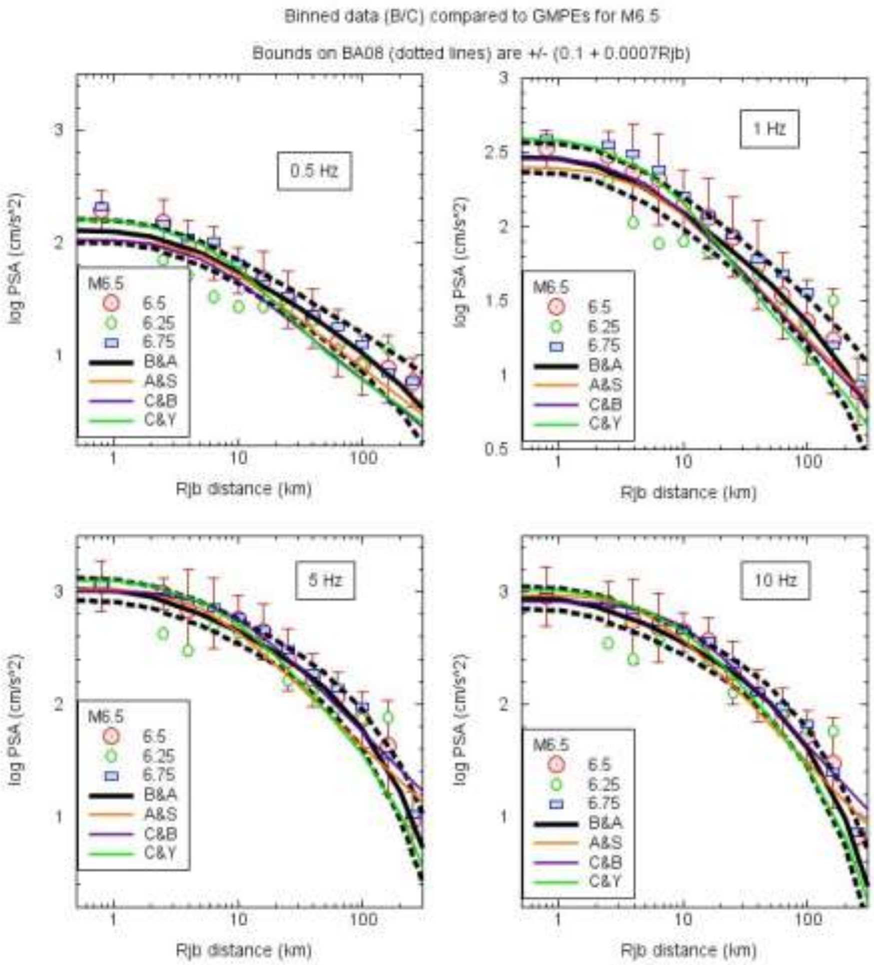

Figure – Proposed median GMPE and epistemic uncertainty bounds for low and high GMPEs (solid and dashed black lines), for crustal events in western Canada.

Western Offshore

As discussed earlier, we may use the crustal GMPEs for offshore events (>50 km offshore), but reduce the magnitude by 0.5 units (to predict lower motions). The uncertainty will be as given for the crustal motions. These events are not a significant contributor to hazard, so a more detailed treatment is not required.

Cascadia interface events

Inspection of plots of alternative GMPEs for interface events (AM09, GA09, Z06), in the magnitude range of interest (**M**8 to 9), reveals a deficiency in their representation of uncertainty (see Appendix C). It just so happens that the 3 GMPEs are very similar at intermediate periods, especially ~2 Hz. And at longer periods they are often quite similar near 100 km, where the major cities are located. Thus the 3 GMPEs do not capture the true epistemic uncertainty - we have never seen one of these events in Cascadia, so the uncertainty in median GMPE cannot possibly be low. Looking closely at the 3 GMPEs for interface events and their attenuation and magnitude-scaling behavior, relative to the BA08' GMPE, to each other, and to the Tohoku data (for fore-arc sites), the AM09 GMPE appears to have the most reasonable behavior. For all magnitudes (7 to 9), it approximately parallels the BA08' GMPE, but is generally about a factor of two higher; thus its attenuation and magnitude scaling are well behaved. Furthermore, it matches the Tohoku data and derived Tohoku regression equation (Ghofrani et al., 2012) quite well for **M**9.

It is perhaps not surprising that the AM09 GMPE would be well behaved, as it is based on simulations for Cascadia attenuation conditions, with the source parameters calibrated from large subduction events in Japan (**M**8.4 Tokachi-Oki). By contrast, the other GMPEs are empirical and suffer from sparse data in the magnitude range of interest – they were developed before the availability of the Tohoku dataset. A recent B.C. Hydro ground-motion study (Abrahamson et al., 2012) also noted the problem with scaling behavior at large magnitudes for many of the subduction GMPEs, and chose to develop new GMPEs for subduction events for this reason. Their developed GMPE for **M**9 interface events is highlighted in red in the figure below; it is quite similar to AM09. (I highlighted the forearc line of BC Hydro – the backarc line is also visible; in their GMPEs the two lines converge at large distances, whereas logically they should converge at short distances.) The B.C. Hydro GMPE and the AM09 GMPE are also similar for **M**=8; overall, the AM09 GMPE has slightly higher amplitudes at 100 km, and attenuates more slowly with distance. The Abrahamson et al. (2012) GMPEs are considered in more detail in Appendix B.

In view of the issues noted above, the initial proposal for epistemic uncertainty in subduction GMPEs is to use the AM09 GMPE as the "central" estimate curve, and define upper and lower representative equations considering other GMPEs. This "sidesteps" the need to adjust empirical GMPEs for Japanese vs. Cascadia site conditions. The plot below, and those in Appendix C, suggest that uncertainty should grow with distance, as was the case for the crustal GMPEs. As the overall uncertainty should exceed that for crustal events, the proposed uncertainty bounds with which to construct upper and lower GMPE curves (relative to AM09) are proposed to be:

Delta (interface) = min((0.15+0.0007 Rcd), 0.35) (log10 units)

This will provide for a factor of 2.8 amplitude scaling from the lower to the upper GMPE, at 100 km (growing to a factor of 5.2 at 300 km).

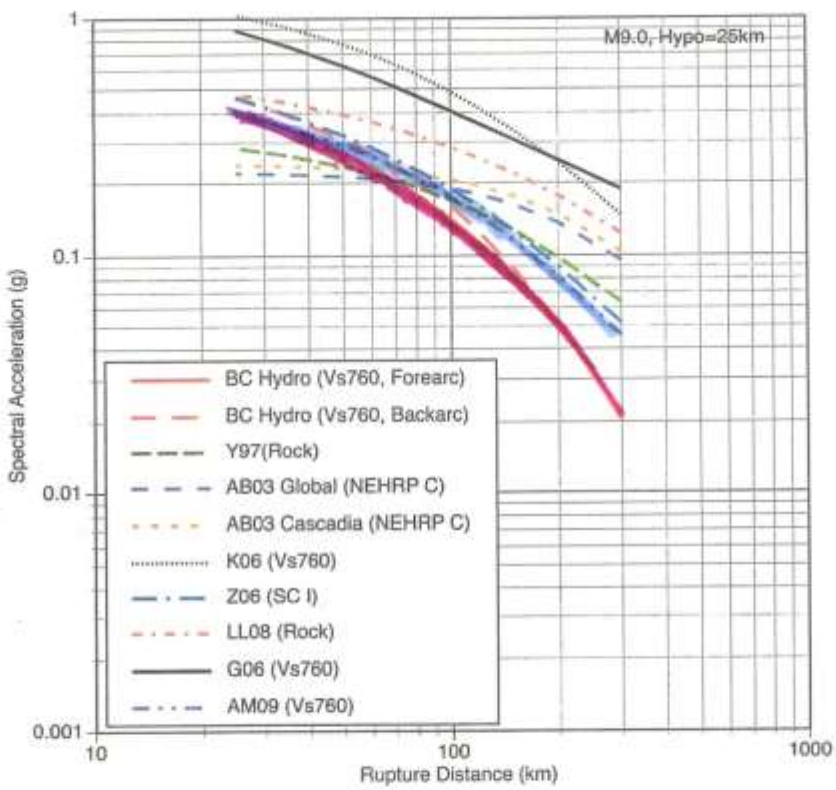

*Figure - T=1 s spectral acceleration for **M**=9 interface events. From B.C. Hydro draft report, used with permission.*

Cascadia in-slab events

The alternative GMPEs for in-slab events suffer from many of the same problems as those for the interface events (also noted in the B.C. Hydro report). The database is sparse for in-slab events of **M**>7, so the magnitude scaling at the upper end of the range for these events (**M**8) is not well constrained. The prevalence of Japanese data in some datasets introduces potentially large amplifications due to shallow soils at higher frequencies, leading to much dispersion between GMPEs developed from different databases. For most of the non-Japanese datasets, the site conditions are poorly known, with limited to no information on standard site metrics such as Vs30. And as noted previously, GMPEs for which Japanese data predominate should be modified (to reduce high-frequency amplitudes and increase low-frequency amplitudes). Amongst the published in-slab GMPEs, the Zhao et al. 2006 equations have the strongest database.

Going through the GMPE plots for in-slab events for **M**=6 to 7.5, after adjustment for Cascadia site conditions, a GMPE uncertainty model is proposed as follows. Use the (Cascadia site adjusted) Z06 GMPE as the "central" estimate, with an uncertainty of 0.15 units – note that it is proposed to use a distance-independent uncertainty, as the Z06 attenuation is very similar to that of AB03 at higher frequencies, which follows that observed during the Nisqually earthquake. So delta = 0.15 (log units); this is about the same as for Cascadia crustal earthquakes, and less than for interface.

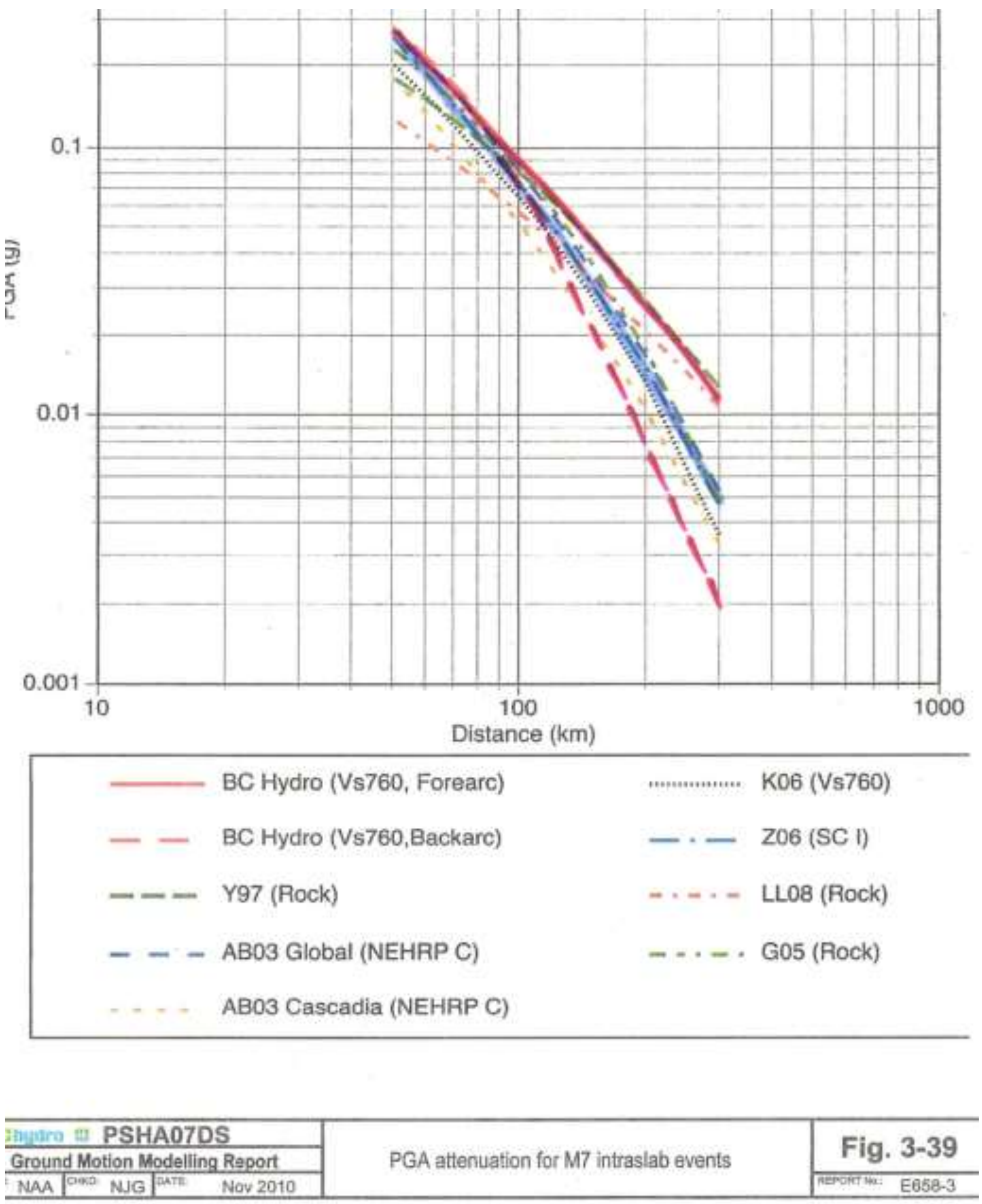

Figure – Comparison of alternative in-slab GMPEs for PGA, for ***M****=7, from draft B.C. Hydro report (reprinted with permission). Note that Z06 GMPE is similar to that developed by B.C. Hydro.*

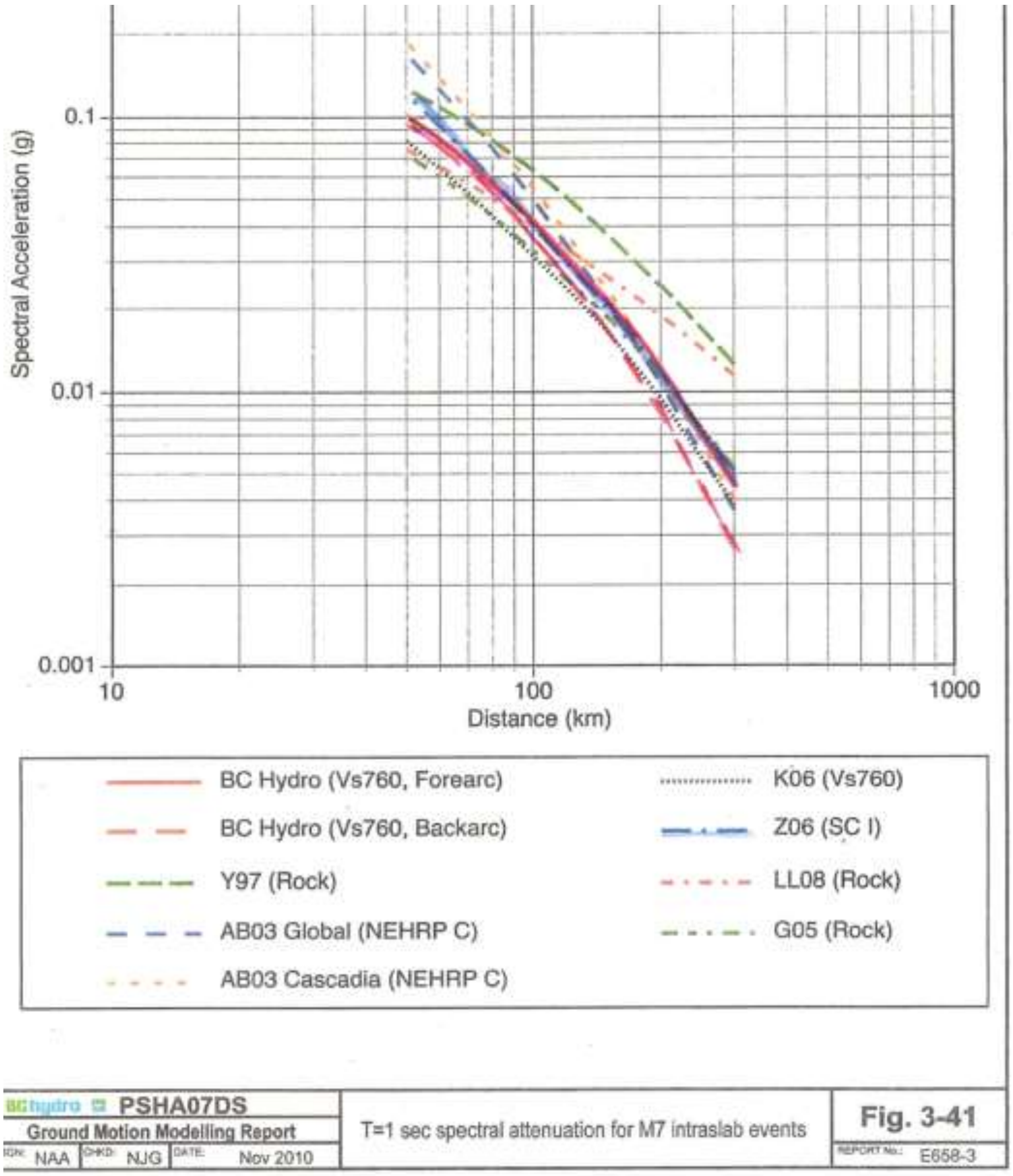

*Figure – Comparison of alternative in-slab GMPEs at T=1 s for **M**=7, from draft B.C. Hydro report (reprinted with permission). Note that Z06 GMPE is similar to that developed by B.C. Hydro.*

Eastern crustal earthquakes

The GMPEs for eastern events as presented above were developed from the median and standard deviation of a suite of 5 GMPEs, all developed using different methods and assumptions. The plots in Appendix C show the suite for **M**4.5, 6.0 and 7.5 at a range of frequencies. In the figure below, the standard deviation of the mean GMPE for the east is plotted versus distance for these three magnitude values, for 0.5 Hz and 5 Hz. Generally, the implied uncertainty from the standard deviation of the GMPEs is larger than the value adopted for western crustal GMPEs, but not always. Overall, the impression is that the eastern GMPEs should carry larger epistemic uncertainty, in comparison to the western crustal equations. Furthermore, in the east the ground motions are most constrained by data and studies at regional distances, and should be considered most uncertain at close distances, due to the paucity of relevant near-source observational data. This uncertainty behavior is different than that for the west. This suggests that additional uncertainty, above that given by the standard deviations of the mean GMPE, should be provided. It is proposed to add an additional epistemic uncertainty that will modify the GMPE+std and GMPE-std equations for the east, having greatest effect at close distances. The uncertainty (log units to add to GMPE+std, and subtract from GMPE-std) is:

Delta (ENA GMPE+std, GMPE-std) = max((0.1 – 0.001 Repi), 0.)

This will increase the epistemic uncertainty above that given by the standard deviation of the mean of the eastern GMPEs by 0.1 (factor of 1.26) at close distances, such that its typical value would be ~0.2 for high frequencies and 0.35 for low frequencies. It would leave the uncertainty unchanged for Repi>100 km. The average value (over all magnitudes and frequencies) is shown in the plot below, in comparison to the western crustal uncertainty.

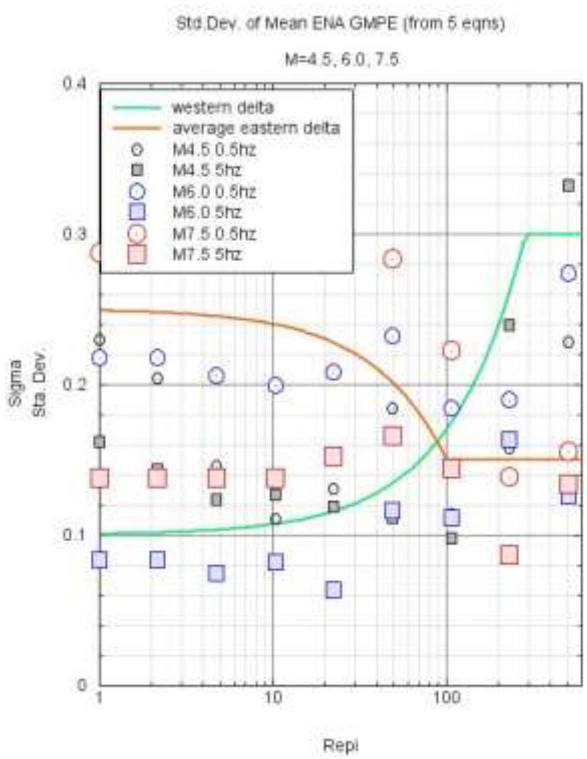

Figure – standard deviation of mean of 5 eastern GMPEs by magnitude and distance for 0.5 and 5 Hz (symbols). Recommended eastern epistemic uncertainty would add 0.1 to these values at close distances (reducing to no addition for Repi>100km). Green line shows recommended epistemic uncertainty for western crustal events. Orange line shows an alternative formulation for eastern epistemic uncertainty (average value independent of magnitude and frequency).

Aleatory Variability in GMPEs (Sigma)

The value of sigma to be associated with the GMPEs is an important parameter. Traditionally, sigma was set based on observed variability about the regression equation (statistics of misfit to the equations). More recently, it has been realized that this may not be the appropriate way to define sigma, as what we are trying to capture is natural variability in future events, as opposed to total variability - which includes factors such as model misfits, variable soil conditions, data errors and so on. These factors all contribute to reported values for regression statistics, but are not representative of actual physical variability. There is also potential for some double-counting of aleatory uncertainty when epistemic uncertainty in the median equations is also included in the hazard analysis. These issues have been discussed in papers by Anderson and Brune (1999), Anderson et al. (2000), Abrahamson and Bommer (2005), Atkinson (2006, 2011) and Strasser et al., (2009). Atkinson (2011) shows that actual variability in amplitudes within well-recorded events is about 0.22 log(10) units at low frequencies (0.3 to 1 Hz), decreasing to about 0.20 units at high frequencies (≥ 4 Hz), for western events. This includes just the within-event variability, and also implicitly includes variability in site conditions for a given value of Vs30 (due to differing soil depths, etc.). Based on the NGA equations, typical inter-event variability values decrease from about 0.16 to 0.12 units over the same frequency range; note this inter-event variability will reflect in part regional variability in source characteristics, in addition to actual event-to-event variability within a specific region. Considering these values, suggested representative values for a multi-site sigma would be about 0.27 log(10) units at low frequencies (≤1 Hz), decreasing to 0.23 units at high frequencies (≥ 4 Hz). These values are obtained from the inter-event and intra-event components using the standard square-root-sum-of-squares rule. It is proposed that these sigma values be applied to all event types and regions, as there is no definitive evidence that sigma varies with region, and sigma is best defined for western crustal events. Moreover, Atkinson (2012) shows that for eastern events, the aleatory variability is similar or smaller to that for western events.

References

Abrahamson, N., G. Atkinson, D. Boore, Y. Bozorgnia, K. Campbell, B. Chiou, I. Idriss, W. Silva and R. Youngs (2008). Comparison of the NGA Ground-Motion Relations. Earthquake Spectra, **24**, 45-66.

Abrahamson, N. and J. Bommer (2005). Probability and uncertainty in seismic hazard analysis. Earthquake Spectra, **21**, 603-608.

Anderson, J. and J. Brune (1999). Methodology for using precarious rocks in Nevada to test seismic hazard models. Bull. Seism. Soc. Am., **89**, 456-467.

Anderson, J., J. Brune, R. Anooshehpoor and S. Ni (2000). New ground motion data and concepts in seismic hazard analysis. Current Science, **79**, 1278-1290.

Assatourians, K., and G. Atkinson (2010). Database of processed time series and response spectra for Canada: An example application to study of the 2005 MN5.4 Riviere du Loup, Quebec earthquake. Seism. Res. L., **81,** 1013-1031.

Atkinson, G. (2006). Single-station sigma. Bull. Seism. Soc. Am., **96**, 446-455.

Atkinson, G. M. (2008). Ground-motion prediction equations for eastern North America from a referenced empirical approach: implications for epistemic uncertainty, *Bull. Seism. Soc. Am.* **98**, 1304-1318.

Atkinson, G. (2011). An empirical perspective on uncertainty in earthquake ground motions. Can.J.Civil Eng., **38**,1-14. DOI:10.1139/l10-120.

Atkinson, G. (2012). Empirical evaluation of aleatory and epistemic uncertainty in eastern ground motions. Seism. Res. L., in press.

Atkinson, G. M., and D. M. Boore (2003). Empirical ground-motion relations for subduction-zone earthquakes and their application to Cascadia and other regions, *Bull. Seism. Soc. Am.* **93**, 1703-1729.

Atkinson, G. M., and R. Casey (2003). A comparison of ground motions from the 2001 **M** 6.8 in-slab earthquakes in Cascadia and Japan, *Bull. Seism. Soc. Am.* **93**, 1823-1831.

Atkinson, G. M. (2005). Ground motions for earthquakes in southwestern British Columbia and northwestern Washington: crustal, in-slab, and offshore events, *Bull. Seism. Soc. Am.* **95**, 1027-1044.

Atkinson, G. M., and D. M. Boore (2006). Earthquake ground-motion prediction equations for eastern North America, *Bull. Seism. Soc. Am.* **96**, 2181-2205.

Atkinson, G. and D. Boore (2011). Modifications to existing ground-motion prediction equations in light of new data. Bull. Seism. Soc. Am., **101**,1121-1135.

Atkinson, G. and K. Goda (2011). Effects of seismicity models and new ground motion prediction equations on seismic hazard assessment for four Canadian cities. Bull. Seism. Soc. Am., **101**, 176-189.

Atkinson, G. M., and M. Macias (2009). Predicted ground motions for great interface earthquakes in the Cascadia subduction zone, *Bull. Seism. Soc. Am.* **99**, 1552-1578.

Atkinson, G. and M. Morrison (2009). Regional variability in ground motion amplitudes along the west coast of North America. Bull. Seism. Soc. Am., **99**, 2393-2409.

Bommer, J. and N. Abrahamson (2006). Why do modern probabilistic seismic hazard analyses often lead to increased hazard estimates? Bull. Seism. Soc. Am., **96**, 1967-1977.

Bommer, J., N. Abrahamson, F. Strasser, A. Pecker, P. Bard, H. Bungum, F. Cotton, D. Fah, F. Sabetta, F. Scherbaum and J. Studer (2004). The challenge of defining upper bounds on earthquake ground motions. Seism. Res. L., **75**, 82-95.

Bommer, J. and F. Scherbaum (2008). The use and misuse of logic trees in probabilistic seismic hazard analysis. Earthquake Spectra, **24**, 997-1009.

Boore, D. and G. Atkinson (2008). Ground-motion prediction equations for the average horizontal component of PGA, PGV, and 5%-damped SA at spectral periods between 0.01s and 10.0 s. Earthquake Spectra, **24**, 99-138.

Boore, D. and W. Joyner (1997). Site amplifications for generic rock sites. Bull. Seism. Soc. Am., **87**, 327-341.

Campbell, K. W. (2003). Prediction of strong ground motion using the hybrid empirical method and its use in the development of ground-motion (attenuation) relations in eastern North America, *Bull. Seism. Soc. Am.* **93**, 1012-1033.

Chiou, B., R. Youngs, N. Abrahamson and K. Addo (2010). Ground motion model for small-to-moderate shallow crustal earthquakes in California and its implications for regionalization of ground motion prediction models. Earthquake Spectra, in press.

Ghofrani, H., G. Atkinson and K. Goda (2012). Implications of the 2011 M9.0 Tohoku Japan earthquake for the treatment of site effects in large earthquakes. Bull. Earthq. Eng., in review.

Ghofrani, H., G. Atkinson, K. Goda and K. Assatourians (2012). Stochastic finite-fault simulations of the 11th March Tohoku, Japan earthquake. Bull. Seism. Soc. Am., in review.

Goda, K., and G. M. Atkinson (2009). Probabilistic characterization of spatially correlated response spectra for earthquakes in Japan, *Bull. Seism. Soc. Am.* **99**, 3003-3020.

Goda, K., H. Hong and G. Atkinson (2010). Impact of using updated information on seismic hazard in Western Canada. Can. J. Civil Eng., **37**, 562-575.

Gregor, N. J., W. J. Silva, I. G. Wong, and R. R. Youngs (2002). Ground-motion attenuation relationships for Cascadia subduction zone megathrust earthquakes based on a stochastic finite-fault model, *Bull. Seism. Soc. Am.* **92**, 1923-1932.

Pezeshk, S., A. Zandieh and B. Tavakoli (2011). Ground-motion prediction equations for eastern North America from a hybrid empirical method. Bull. Seism. Soc. Am., in review.

Power, M., Chiou, B., Abrahamson, N, Y. Bozorgnia, T. Shantz and Roblee, C. (2008). An overview of the NGA project. Earthquake Spectra, **24**, 3-21.

Ristau, J., G. C. Rogers, and J. F. Cassidy, (2003). Moment magnitude-local magnitude calibration for earthquakes off Canada's west coast, *Bull. Seism. Soc. Am.* **93**, 2296- 2300.

Ristau, J., G. C. Rogers, and J. F. Cassidy (2005). Moment magnitude-local magnitude calibration for earthquakes in western Canada, *Bull. Seism. Soc. Am.* **95**, 1994-2000.

Scherbaum, F., J. Schmedes, and F. Cotton (2004). On the conversion of source-to-site distance measures for extended earthquake source models, *Bull. Seism. Soc. Am.* **94**, 1053-1069.

Silva, W. J., N. J. Gregor, and R. Darragh (2002). *Development of regional hard rock attenuation relations for central and eastern North America*, Technical Report, Pacific Engineering and Analysis, El Cerrito, CA.

Somerville, P., N. Collins, N. Abrahamson, R. Graves and C. Saikia (2002). Ground motion attenuation relations for the central and eastern United States. Report to U.S. Geological Survey (NEHRP).

Strasser, F., N. Abrahamson and J. Bommer (2009). Sigma: Issues, insights and challenges. Seism. Res. L., **80**, 40-56.

Youngs, R. R., S. J. Chiou, W. J. Silva, and J. R. Humprey (1997). Strong ground motion attenuation relationships for subduction zone earthquakes, *Seism. Res. Lett.* **68**, 58-73.

Zhao, J. X., J. Zhang, A. Asano, Y. Ohno, T. Oouchi, T. Takahashi, H. Ogawa, K. Irikura, H. K. Thio, P. G. Somerville, Y. Fukushima, and Y. Fukushima (2006). Attenuation relations of strong ground motion in Japan using site classification based on predominant period, *Bull. Seism. Soc. Am.* **96**, 898-913.

Appendix A: Finite-fault to Point-Source Distance Conversion Approximation

For the 2015 national hazard maps, the computation software is based on a point source for areal sources, in which events happen at their focus, and the distance measure from a site to an event is the epicentral distance (Repi), converted to hypocentral distance (Rhypo) via focal depth where appropriate. By contrast most GMPEs (ground-motion prediction equations) now give motions for a finite fault measure, either Rcd (closest distance to rupture plane) or Rjb (Joyner-Boore distance, closest distance to surface projection of rupture plane). There have been several studies on how to do conversions between Rcd or Rjb and Rhypo or Repi (eg. Scherbaum, Goda). In this appendix a simple alternative conversion is outlined, that may serve as an adequate approximation. It has two advantages over other conversions: (i) it is very simple to apply; and (ii) it is easy to adjust to allow application for ENA (eastern) fault parameter models, which differ from those in the west, or to consider any desired focal depth. An approximation for in-slab events is also provided. Note that no approximation is required for interface events as we know the geometry of these sources.

The way the approximation is implemented is as follows: the software is working in terms of Repi, so the value of Repi should be converted to the appropriate distance measure before looking up the corresponding ground motion value from the GMPE look-up tables (which may be given in terms of Repi, Rhypo, Rcd or Rjb).

Proposed Approximation for Crustal Events

We estimate the fault length (L) and width (W) for western settings from the classic formulae of Wells and Coppersmith (1984), where M is moment magnitude:

$$L(west) = 10^{(-2.44 + 0.59 M)} \quad (1)$$

$$W(west) = 10^{(-1.01 + 0.32M)} \quad (2)$$

Following Atkinson and Boore (2006) (who quote Somerville on this point), these dimensions should each be multiplied by a factor of 0.6 for eastern sources, as they are smaller:

$$L(east) = 0.6L(west) \quad (3)$$

$$W(east) = 0.6W(west) \quad (4)$$

We assume that, on average, hypocenters are located at the centre of the fault plane. For geometric simplicity, we assume a vertical fault plane. In this case, the depth to the top of the rupture (Dtop) is:

$$Dtop = h - 0.5W \quad (5)$$

where h is the focal depth (and W is either W(west) or W(east) as appropriate). If we are using the AB06' GMPE, note that a minimum distance Ztor has been recommended to force near-source saturation, as given by:

Ztor(AB06') = 21. -2.5M (6)

Thus if we are using AB06' (and only for AB06'), we would replace Eqn(5) with:

Dtop = max(Ztor(AB06'), (h-0.5W)) (7)

Finally, we need to ensure that the depth to the top of rupture is never less than 0. So the vertical distance from the surface down to the top of our fault is:

Ztor = max(Dtop, 0) (8)

Our fault plane is a line in map view (because it's vertical), placed at a depth (for the top of the plane) as given by Equation (8). Since the epicentre has been assigned to the middle of the fault, which has length L, the nearest distance of a point to the surface projection of the fault line would range from a minimum of (Repi – 0.5 L) for an azimuth of 0 with respect to the fault, to a maximum of (Repi) for an azimuth of 90 degrees (with the constraint that it cannot be less than Repi=0.1). The average value, by calculating the average of cos(azimuth) from 0 to 360 degrees, and including the constraint, will be:

Dsurf = max((Repi – 0.3 L), 0.1) (9)

Equation (9) gives us the average distance to the fault projection in the horizontal plane. So, if the GMPE table is given in terms of epicentral distance, we use:

Repi = Repi (10)

If the GMPE table is given in terms of hypocentral distance we use:

Rhypo = sqrt(Repi*Repi + h*h) (11)

If the GMPE table is given in terms of Rcd we use:

Rcd = sqrt(Dsurf*Dsurf + Ztor*Ztor) (12)

If the GMPE table is given in terms of Rjb we use:

Rjb = Dsurf (13)

We tested how well this works by running a sample seismic hazard calculation problem for a moderate hazard environment, using the AB06 GMPE in Rcd, with Eqn (12) used to convert Repi to Rcd. We compared the results to those obtained by using a version of AB06 that was developed by regressing the simulated PSA against Rhypo instead of Rcd (so that the AB06 GMPE was given directly in Rhypo). We got the same expected ground motion values at probabilities down to $\sim 10^{-4}$, to within about 5%. We also tested the impact of this approximation on hazard results relative to more complicated and detailed formulations such as that proposed by Goda and Atkinson. Again, we find the hazard results are insensitive to the details of the selected conversion geometry.

Proposed Approximation for In-Slab sources

Strasser et al. (2010, SRL) provide equations similar to the Wells and Coppersmith relations, for in-slab events. The area from Strasser et al. is:

$$\text{Log } A = -3.225 + 0.89\,\mathbf{M} \qquad (14)$$

We assume that the in-slab sources can be represented by a circular areal projection on the surface, about 50 km above the subducting slab, with radius r_i. This is a reasonable approximation: for example, the area given by Equation (14) for an event of **M**7.2 leads to a radius of r_i = 22km, or an equivalent "fault length/width" of 44km. If we use the equations of Strasser et al. to estimate both the length and width for this magnitude, we obtain a slip size of 49 by 31 km. Assuming an epicentre in the centre of the fault, the value of r_i is the amount by which the epicentral distance needs to be reduced to find the closest distance to the surface projection of the rupture (with the constraint that this distance cannot be <0).

The closest-distance to the fault for in-slab events can thus be calculated within the hazard software from the epicentral distance with the approximation:

$$Rjb = \max((Repi - r_i), 0)$$

$$Rcd = \sqrt{(Rjb^2 + h_{slab}^2)} \qquad (15)$$

where h_{slab} is the depth of the slab.

Appendix B: Sensitivity of NBCC2015 proposed ground motions to use of "3-representative equation" approach to epistemic uncertainty, in comparison to "suite of alternative GMPEs" approach

A point raised by the Reviewer (Paul Somerville) of the proposed 2015 NBCC national hazard maps concerns the use of 3 representative equations to represent epistemic uncertainty, rather than the direct use of the alternative GMPEs (ground-motion prediction equations) from which the suites were derived. He also recommends specific GMPEs that he advises be considered (Table 1 of his review).

The underlying issue is illustrated in the figure below, for the case of eastern GMPEs. We considered the 5 alternative GMPEs shown, but chose to develop a model of epistemic uncertainty that was based on a "3-representative equation" representation. We used the 5 equations as a guide to developing our model, using in this case the mean and standard deviation of the 5 equations as an initial estimate of uncertainty (as the 5 equations have very different magnitude-distance behaviour, especially at lower frequencies). We subsequently refined the uncertainty bounds as described in the White Paper. We note that the details of the approach for developing the 3 representative equations varied with region/event type. For some event types there was a reasonable "representative" equation for which bounds could be specified to encompass the alternatives (e.g. western crustal GMPEs); the development of the representative equations is more straightforward in such a case.

The representative equation approach was selected because it has several advantages from the perspective of national seismic hazard mapping: 1) it allows us to control the applied epistemic uncertainty based on our judgements of the uncertainties in each region in a flexible way; 2) it allows us to rationalize the amount of applied epistemic uncertainty across event types and regions to ensure internal consistency with knowledge and data constraints; and 3) it allows us to simplify the logic tree to a manageable configuration for GSCFrisk;. As noted by Paul Somerville, a potential draw-back of the approach is that it contains a significant subjective element, representing the opinions of the ground-motion working group concerning the best central GMPE and its bounds.

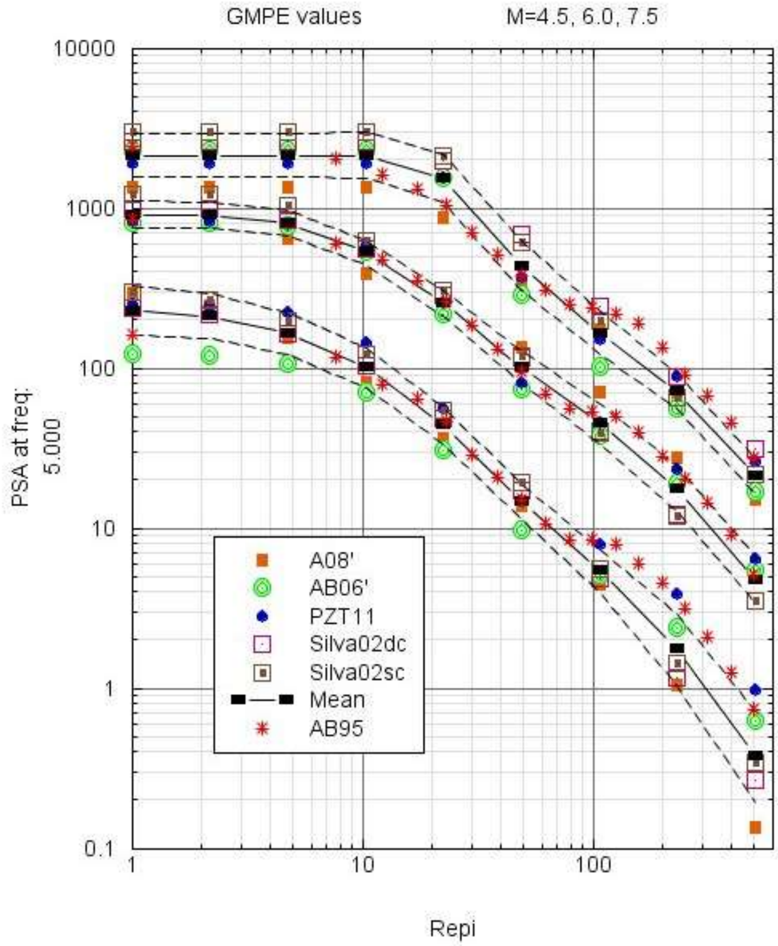

*PSA values at 5Hz (**M**=4.5, 6.0, 7.5) for 5 ENA GMPEs versus epicentral distance, along with geomean values (black squares), and relations giving mean±standard deviation. Red asterisks show AB95 equations used in 2005, 2010 NBCC maps.*

Paul Somerville points out that the standard practice is to use alternative equations, and suggested that we should follow this approach, picking three to four equations for each region/event type as noted in his Table 1. Because we prefer the use of the representative equation approach, as noted above, we have chosen to address this recommendation through the use of a sensitivity test. Specifically, we want to confirm that our approach is generally comparable to the use of the alternative equations as recommended by Paul.

We selected one region for a detailed sensitivity test – the East - due to limited time and resources. Additionally, using insights gained from this test, we double checked all equations and their bounds to ensure that the GMPEs recommended in Paul's Table 1 are accommodated in our approach, and made recommendations for changes to consider where warranted.

Detailed Sensitivity Test

We tested the sensitivity of the hazard curves for 5 eastern cities (Toronto, Montreal, La Malbaie, Quebec City, Ottawa, all for B/C site conditions) to the treatment of epistemic uncertainty. We used the

EQHaz software (Assatourians and Atkinson, 2012; www. Seismotoolbox.ca) to perform the computations, as it can handle 5 alternative GMPEs. We used the input source models as proposed by the GSC (with 50% weight each for the historical and hybrid models, and with magnitude recurrence parameters and weights as given by the GSC). For the GMPEs, we compared two alternatives: 1) with the 3-equation bounds as proposed in the White Paper, weighted at 0.5, 0.25, 0.25 (mid, low, high); and 2) with the 5 alternative equations, equally weighted. The hazard curves for these cases are compared for 5 cities in the following plots. In general, the results are very similar, with our representative approach yielding slightly larger ground motions at most periods. **At the 1/2500 p.a. probability level, differences between the ground motions predicted by the two approaches are <10% at all frequencies for all 5 cities, and <5% in most cases.** For example, one of the larger differences noted is for PGA at Quebec City, for which the 3-representative equation approach differs from the use of 5 equations by 7%. Differences between the approaches tend to grow at low probabilities, which are sensitive to the distribution of epistemic uncertainty.

Plot Set 1: 5 Alternative Equations Equally Weighted, Vs. 3 Representative Eqns (0.5, 0.25, 0.25)

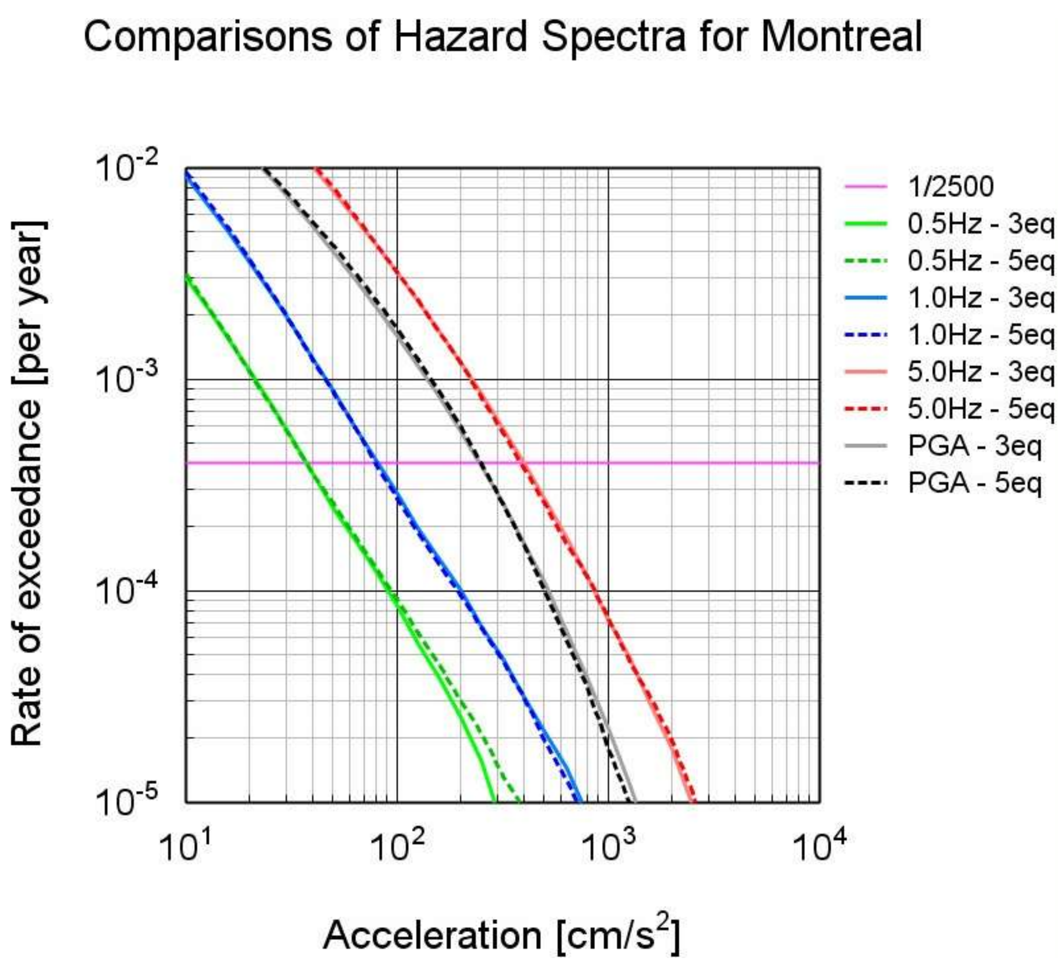

Comparisons of Hazard Spectra for Ottawa

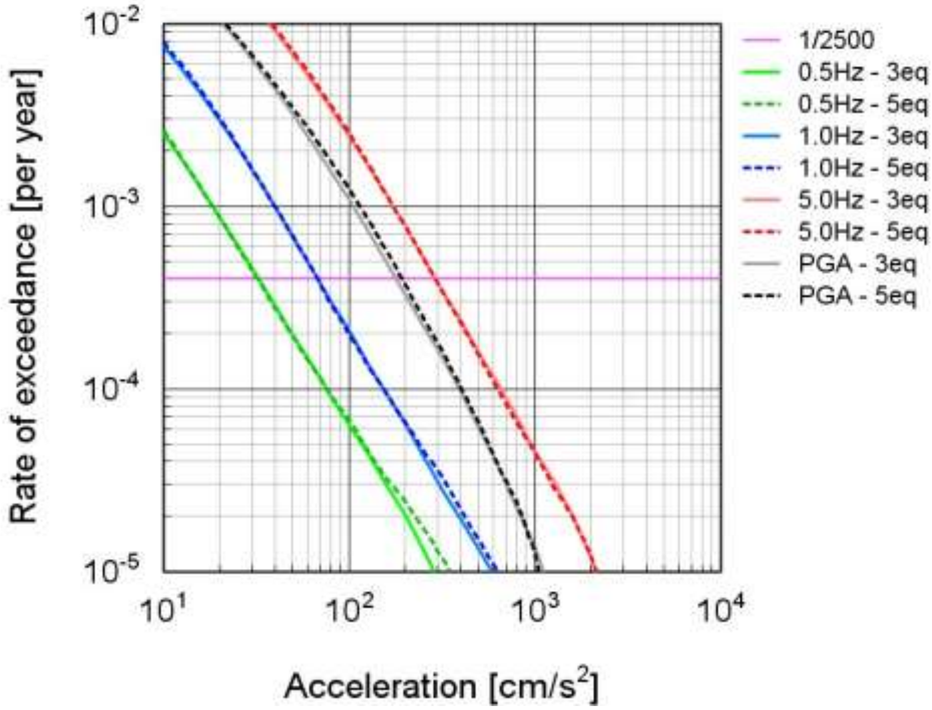

Comparisons of Hazard Spectra for Quebec City

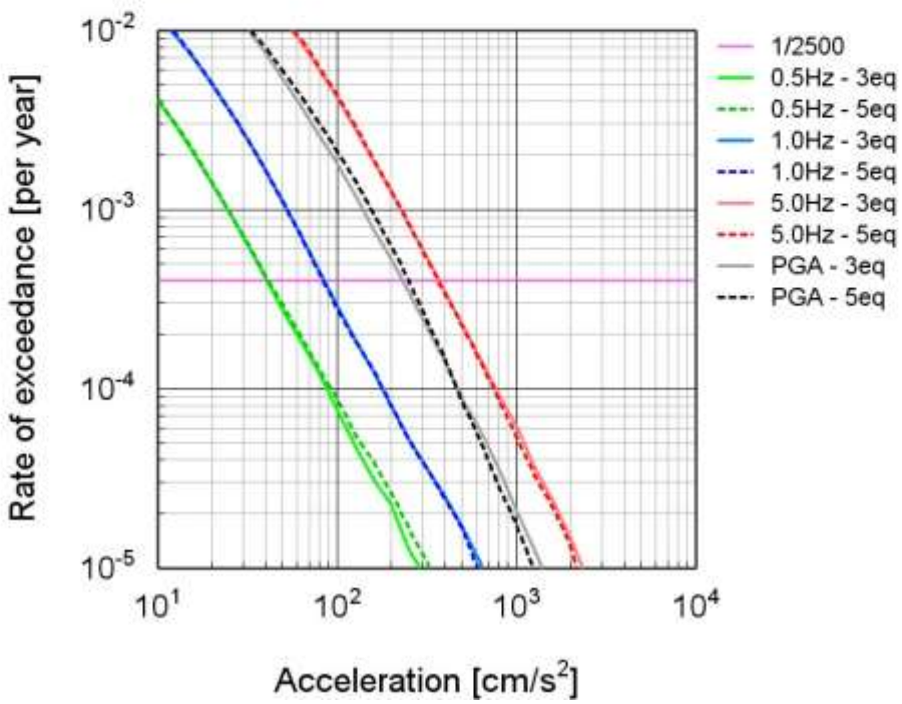

Comparisons of Hazard Spectra for Toronto

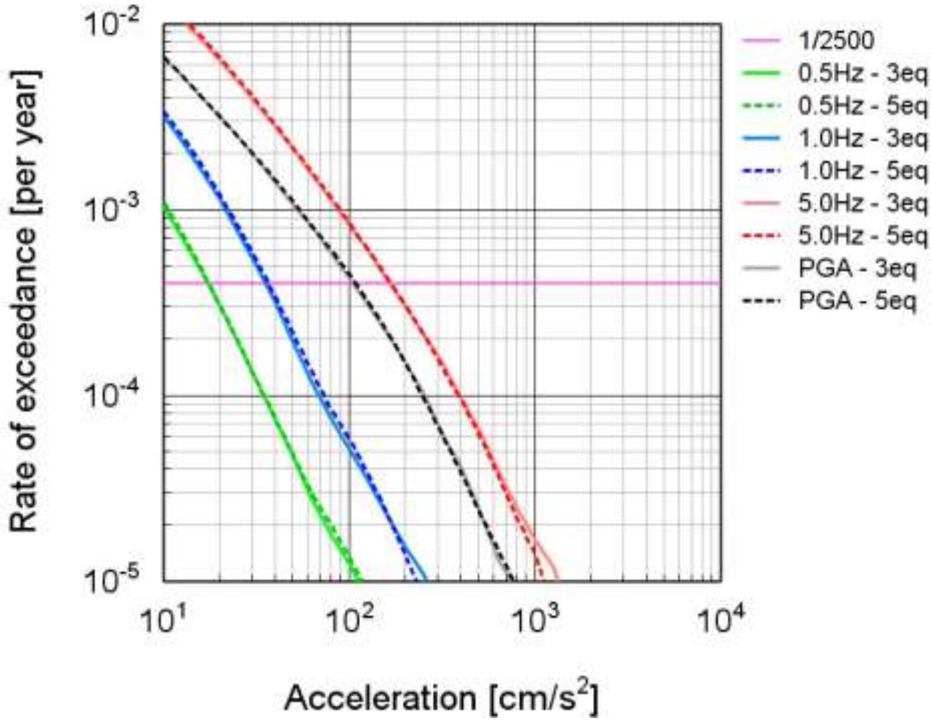

Comparisons of Hazard Spectra for La Malbaie

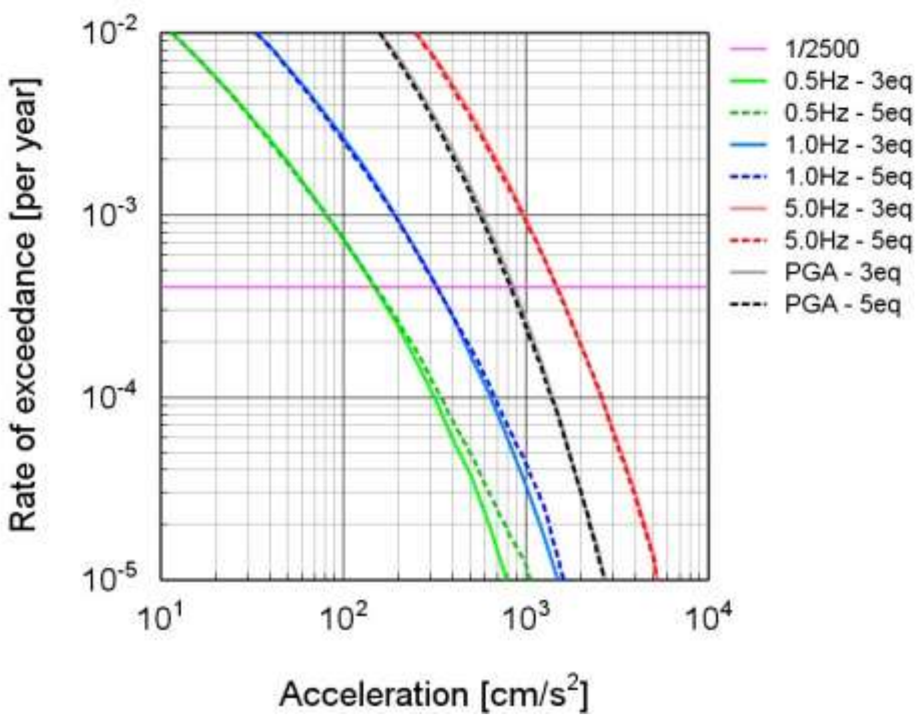

Paul's recommended suite

We also tested the effect of changing the weights for the 5 alternative equations to weights of 0.25 for A08', AB06', PZT11, SilvaDC, 0 for SilvaSC; this eliminates the SilvaSC model to consider just the 4 models recommended by Paul Somerville (Paul expressed reservations regarding the conservatism of the SilvaSC model). This case results in larger differences, because the SilvaSC model is generally the most conservative, so eliminating it reduces the predicted motions, especially at longer periods. This comparison illustrates that the choice of models that are considered is more important than whether the models are run individually or considered collectively through the use of representative equations. The plots are shown below. Overall, we conclude that the effect of using the representative equation approach rather than individual GMPEs is not significant, but that the choice of the equations being considered is important. Our approach may be somewhat conservative in terms of the predicted ground at lower frequencies (1 Hz and lower) in the East, due to our inclusion of the conservative single-corner model of Silva et al., 2002 as a considered GMPE for the derivation of the representative equations. This conservatism was intentional on our part as we believe the epistemic uncertainty in ENA ground motions is relatively large, and we included the single-corner model to more fully consider it.

Plot Set Two: Giving 0-weight to the S02SC model

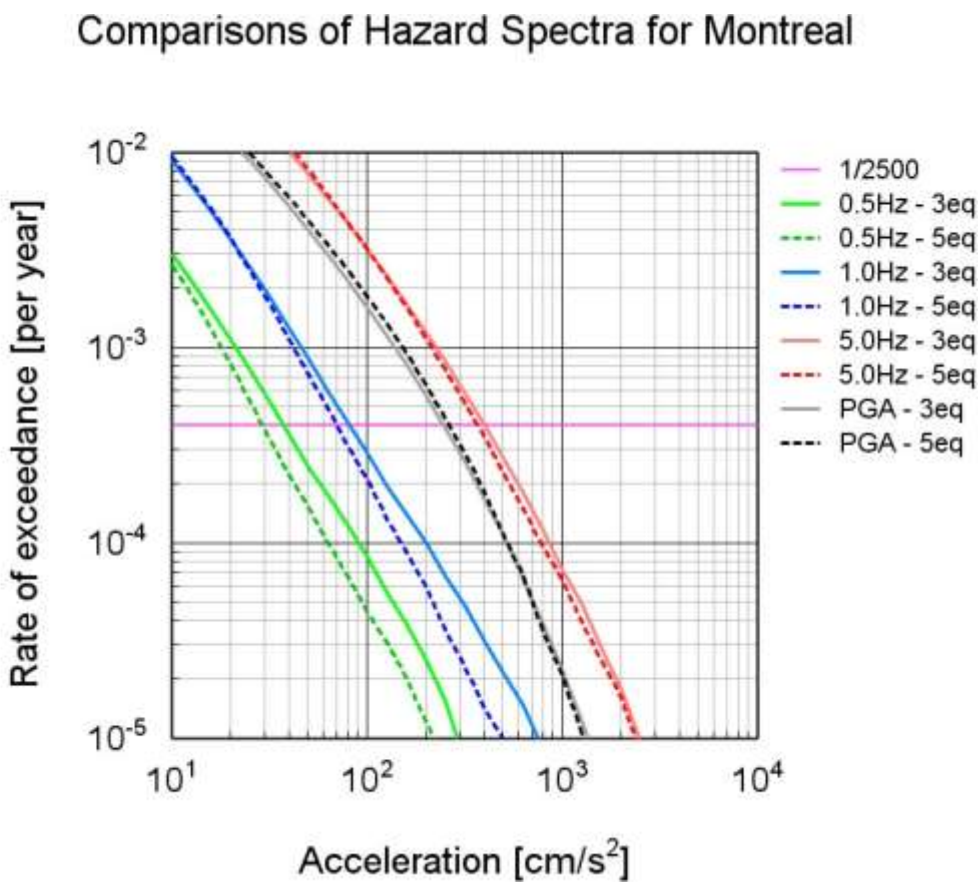

Comparisons of Hazard Spectra for Ottawa

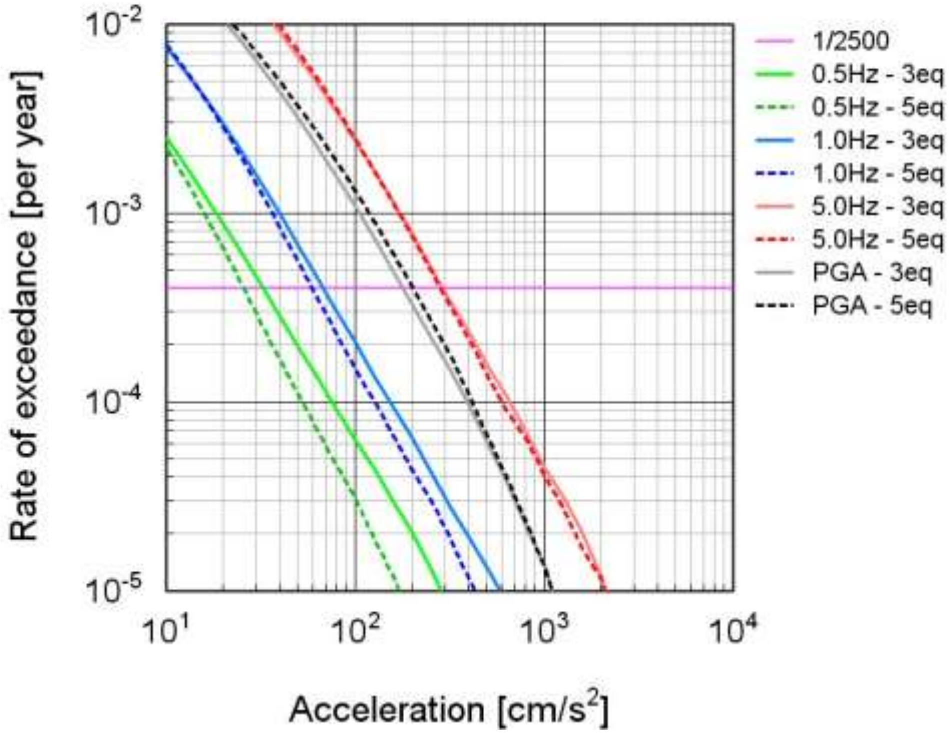

Comparisons of Hazard Spectra for Quebec City

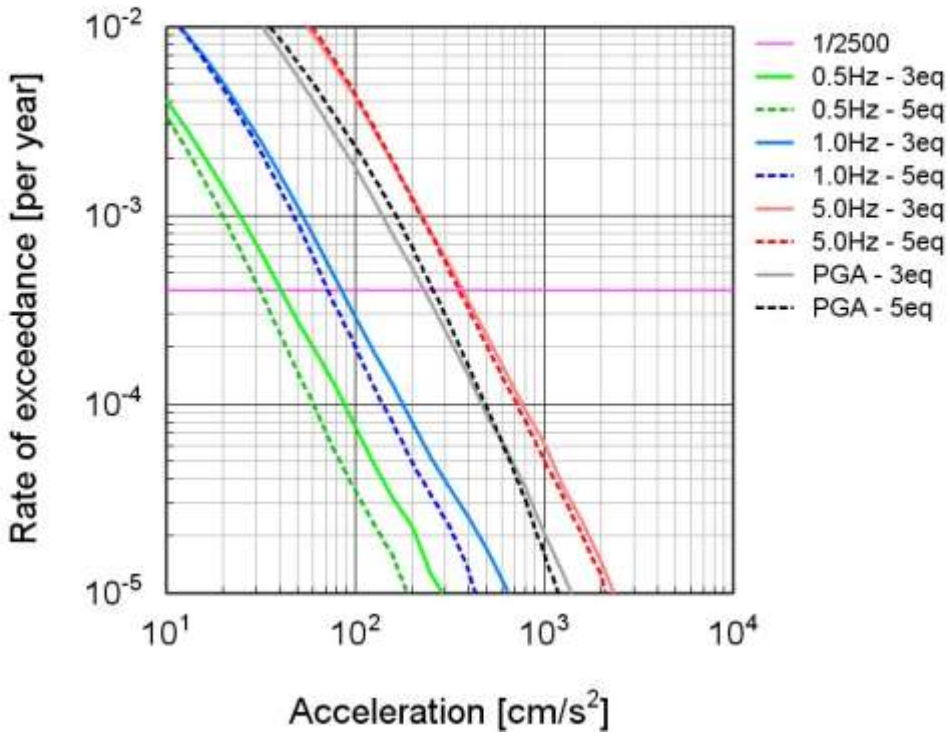

Comparisons of Hazard Spectra for Toronto

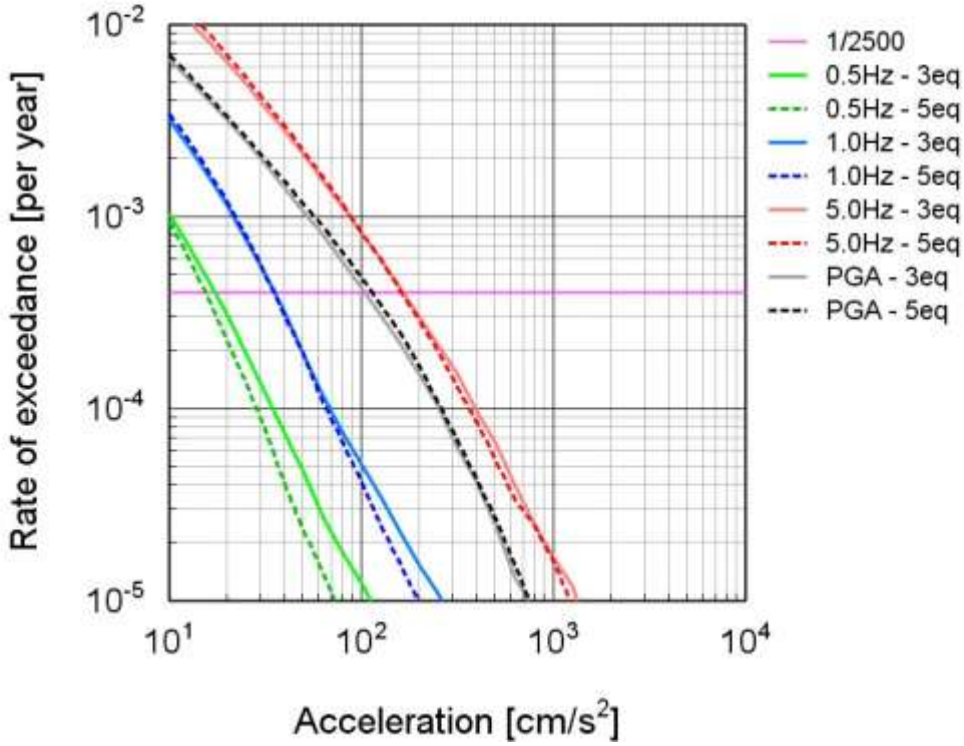

Comparisons of Hazard Spectra for La Malbaie

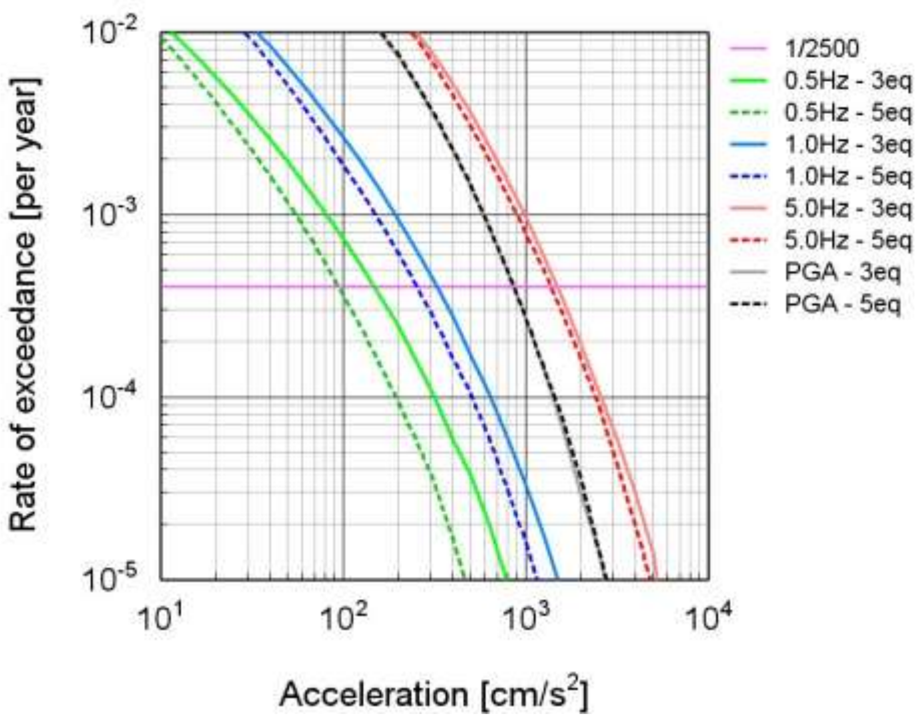

We conclude that the representative equation approach is comparable to the use of alternative equations from which the bounds were derived. If the weights for the included selection are consistently selected, the results are nearly the same. For representative equations that approximately encompass the alternative GMPEs, assuming weights of 0.5, 0.25, 0.25 for the mid, low and high equations reproduces the mean hazard curves that would be obtained using equivalently-weighted alternative equations directly. As pointed out by Paul Somerville, there is a significant subjective element involved in the selection and weighting of GMPEs (this is true regardless of how they are derived). In view of the sensitivity exercise, we conclude that the representative equations should approximately encompass the GMPEs that we wish to accommodate. In the next section, we check whether this condition is met for the GMPEs recommended by Paul.

Checks on GMPEs for Important Event Types

In the following, we check whether the representative equations encompass the GMPEs recommended by Paul Somerville for each event type of interest.

1 – ENA Events

The four ENA GMPEs recommended for consideration by Paul Somerville are A08’, AB06’, PZT11 and S02dc; these are four of the five GMPEs used in deriving the mid GMPE and its range (the upper and lower representative equations are labelled “bounds” in the figure below). The fifth GMPE, the S02sc model is considered by Paul to be inappropriate for inclusion because it may be overly conservative for larger events (it does not use a finite-fault model). The figure below plots the ratio of each of these four equations to the adopted mid-GMPE for ENA, for magnitudes 5.5 to 7.5. The corresponding ratios for the low and high representative equations are also shown. It is interesting that the effect of our inclusion of the S02sc model in our development is clearly manifested in this figure. Our upper representative equations tend to be on the high side relative to the four GMPEs recommended by Paul (as also seen in the previous hazard plots). This is because the upper representative equations were significantly influenced by the S02sc model. We agree with Paul Somerville that this model may indeed be overly conservative, and thus our upper representative equations may be conservative. However, we have elected to retain this conservatism for two reasons: 1) the inclusion of a single-corner stochastic model is consistent with the USGS and industry practice in the U.S.; and 2) there is an overall concern in SCED, with which the Ground Motion Group concurs, regarding the uncertainty in ENA ground motions. We have therefore taken special care to ensure the uncertainty is not underestimated. Thus we choose to retain the recommended range, while acknowledging that the upper equation may be conservative – this is the nature of epistemic uncertainty. The sensitivity test indicates that the amount of conservatism expected due to this decision is not unreasonably large.

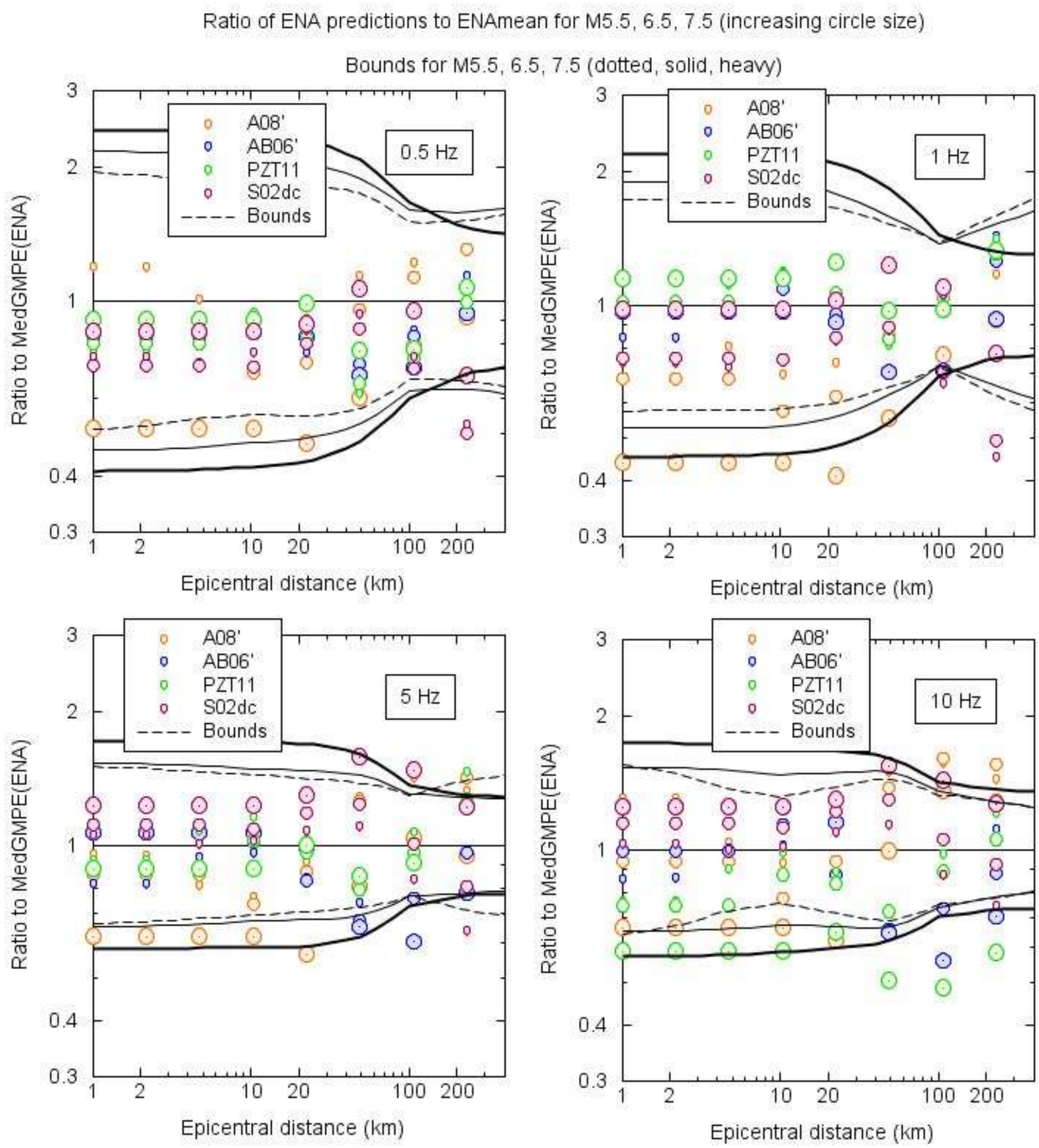

2 – Western Crustal event types

The recommended GMPEs to consider are the 4 PEER-NGA eqns of BA08, AS08, CB08 and CY08 (as per the Somerville review report). As shown below, the representative equations approximately encompass these equations for the magnitude-distance range important to hazard (M6.5 to 7.5 at <100 km). Note that we have deliberately widened the uncertainty in some distance ranges to account for epistemic uncertainty suggested by the data that is not captured by the alternative GMPEs.

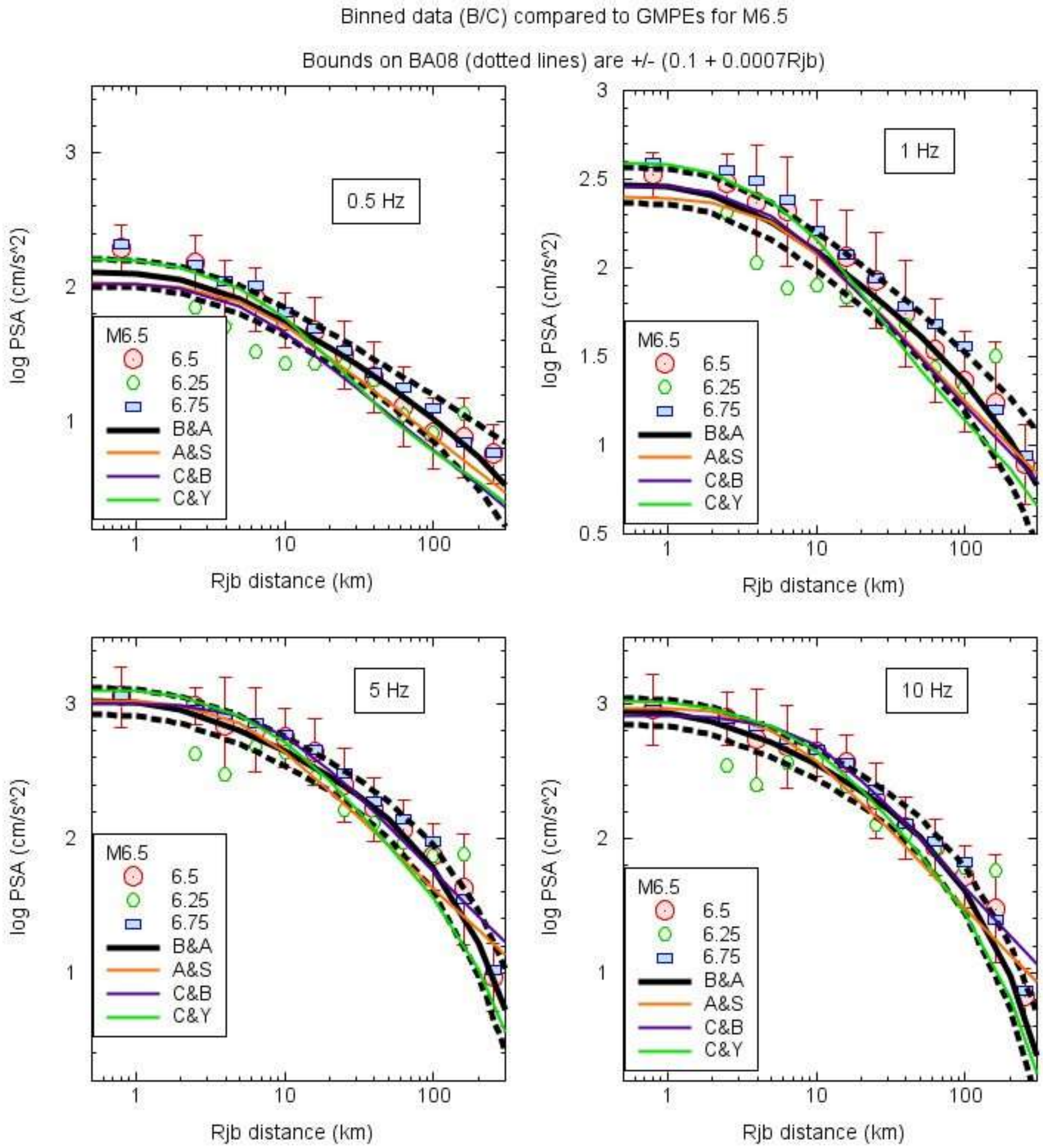

Binned data (B/C) compared to GMPEs for M6.5
Bounds on BA08 (dotted lines) are +/- (0.1 + 0.0007Rjb)
0.5 Hz
1 Hz
5 Hz
10 Hz
log PSA (cm/s^2)
Rjb distance (km)
M6.5
6.5
6.25
6.75
B&A
A&S
C&B
C&Y

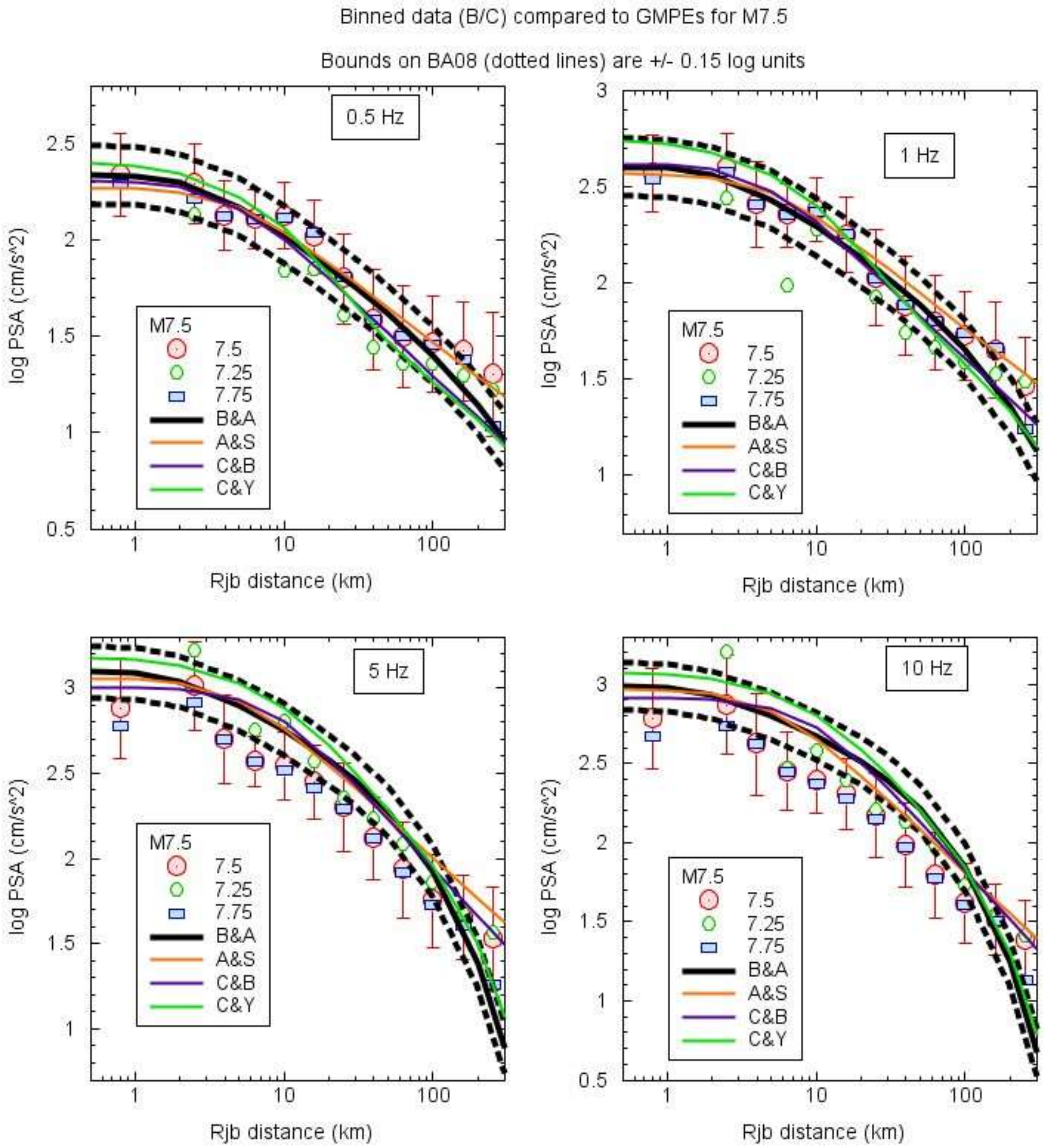

To further explore the potential overall effect of using BA08' as the central equation, the figure below plots the ratios of the other NGA equations' to the BA08' predictions; the ratios to BA08' for the representative equations are also shown. This shows that all of the NGA equations predict very similar motions at near-source distances, for M5.5 to 7.5, at all frequencies. There is a tendency for the other NGA equations to predict motions ~20% higher than BA08 at distances ~5km; this trend reverses as distance increases such that BA08 tends to predict ~20% higher at 50 km. At larger distances the values scatter more widely with no particular trend. The representative equations encompass the ratios, except for M5.5 events at 5 Hz in the distance range from 1 to 20 km. It is noted that the sensitivity of results to this potential bias could be tested by running an alternative hazard calculation that places greater weight on the upper representative curve than on the lower representative curve (e.g. 0.5, 0.3, 0.2 for mid, high, low).

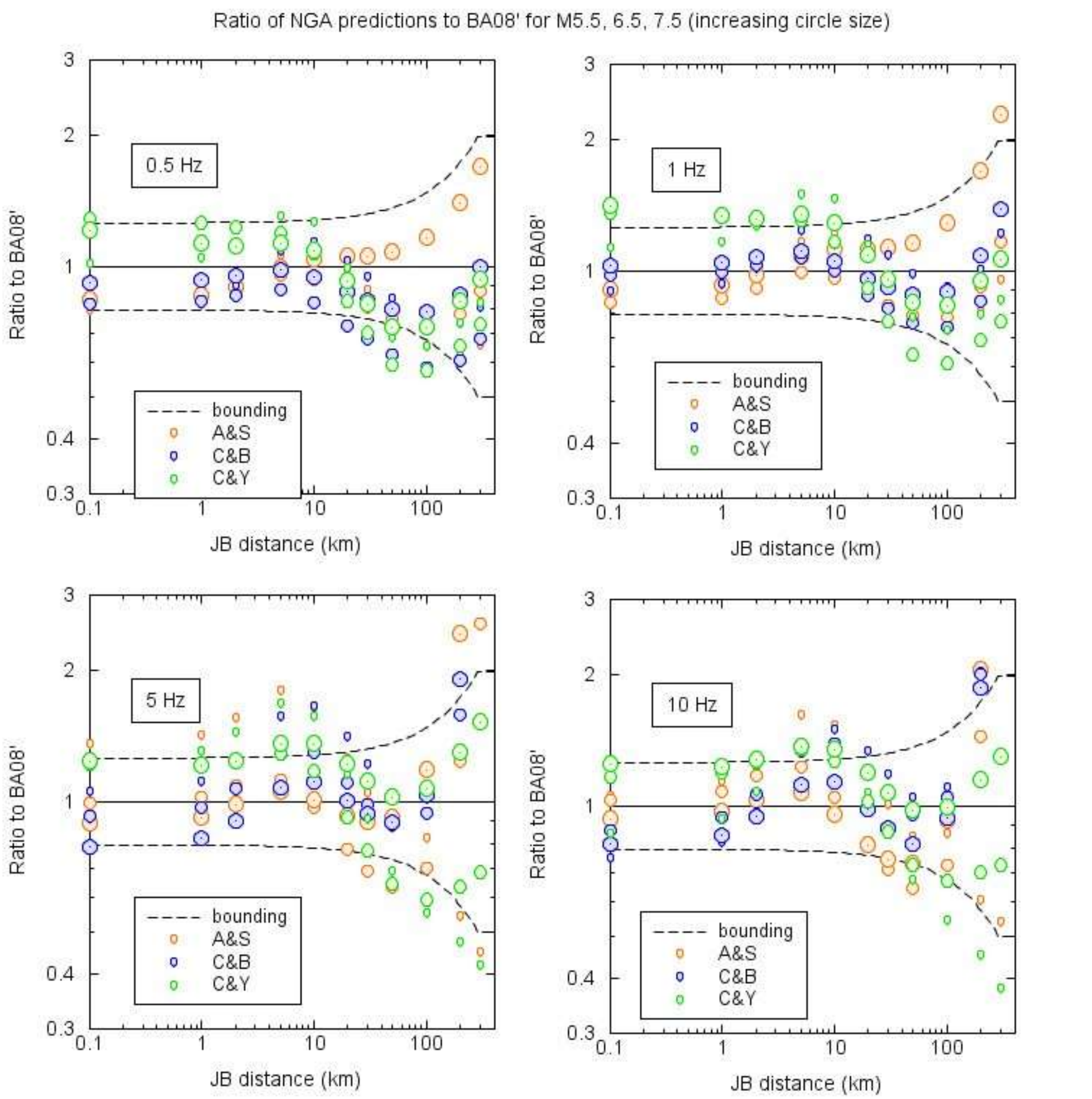

3 - Western In-Slab Events

The GMPE issues are more complex for in-slab and interface events due to the lack of suitable GMPEs for such events in the Cascadia region. As noted in the White Paper, there is a significant bias in GMPEs that include large amounts of data from Japan, due to the significant high-frequency site effects that are caused by the shallow soil conditions there. This characteristic of Japanese data is now well known and has been discussed by a number of researchers (see the White Paper, and the Note on B/C to C conversions), but has not to date been adequately accounted for in the development of GMPEs. It has been recently quantified in Ph.D. work by Ghofrani; the figure below gives an appreciation of the significance of the effect by plotting average site amplification factors for Japan (based on analysis of hundreds of thousands of surface and borehole records, including those from Tohoku). Note that Class C sites in Japan, on average, amplify motions in the 5 to 10 Hz band by a factor of about 3 relative to the B/C reference condition (dashed line in figure; amplification ~1). By contrast, in-slab data recorded in Cascadia have shown larger amplifications at low frequencies, and less amplification at high frequencies (Atkinson and Casey, 2003; Atkinson and Boore, 2003). Because these effects are so significant, we believe that they must be addressed in the implementation of GMPEs for subduction events (as described in the White Paper). No published GMPEs based on global datasets have yet addressed this issue in a satisfactory way. Nor do the recently-submitted Abrahamson et al. 2012 GMPEs for in-slab and interface address this issue. Abrahamson et al. note that their global model overpredicts high-frequency motions for Cascadia by a factor of ~1.5; we believe the reason for this is the regional site factor effect. The importance of regional site corrections is further supported by the current NGA-West2 developments, in which region-specific site correction factors are now being developed in a general way.

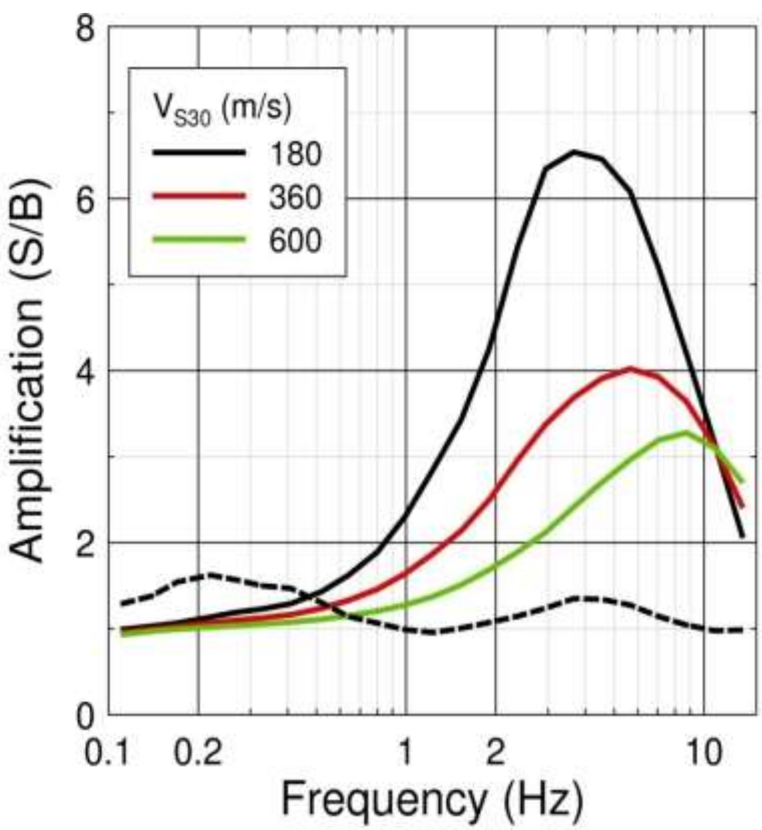

We acknowledge that the influence that regional adjustment factors, in particular for the site conditions, have for our in-slab GMPE suite is troubling, and an additional source of uncertainty, as pointed out by Paul Somerville. We have chosen to address this concern by taking a second look at the proposed

GMPE suite and its representative range, relative to the relevant data. For the Cascadia region, the best data are from the 2001 **M**6.8 Nisqually earthquake (in-slab event, depth=50km). These data, taken from Atkinson and Boore (2003), have **NOT** been adjusted to B/C site conditions, in view of the uncertainty as to how this adjustment should be done for the Cascadia region (see separate document provided on B/C to C conversions). Thus it is important to recognize, when reviewing these data, that motions on C or D should potentially be de-amplified by factors of 1.5 to 3 to represent B/C. We supplement the Cascadia data by considering also data from similar events in Japan, with the amplitudes adjusted to B/C conditions as described in Atkinson and Casey (2003) for the 2001 event, or the recent work of Ghofrani (Ph.D. thesis) for events in 2003 and 2008. The following plot shows the medium, low and high GMPE equations proposed for in-slab events of **M**6.8 on B/C (at a focal depth of 50 km) in comparison to relevant data. Of course, the Nisqually data are the most important. Of the Japanese events, the 2001 event is the most relevant because it has a similar focal depth (50 km) to the Nisqually event. High-frequency motions from the 2003 **M**6.8 event in Japan will have been enhanced by its deeper hypocentre (108 km), while amplitudes at all frequencies for the 2008 **M**7.0 event in Japan (depth 71 km) should be greater than the predictions for **M**6.8 due to the magnitude effect (this represents a shift in the vertical axis by a factor of ~1.5).

For in-slab events, Paul Somerville recommends considering the Zhao et al, 2006 GMPE and the Abrahamson et al., 2012 GMPE. Our representative equations are based on Zhao (our "middle" equation is Zhao, 2006, corrected to B/C site conditions in Cascadia), so they are already considered. We add the Abrahamson et al. equation in the comparison plot, along with the relevant data.

In viewing the plot, we note that our middle equation is very similar to Abrahamson et al at 1 Hz. Our equation is higher at low frequencies, and lower at high frequencies, in comparison to Abrahamson et al. We believe the main reason for the difference is probably the effect of regional site conditions as noted above. In comparison to the plotted data, our proposed suite appears to be justified for the Nisqually and 2001 **M**6.8 Japan event at all frequencies, while at higher frequencies our suite appears to be "too low" for the 2003 **M**6.8 and 2008 **M**7.0 event (though note the caveats mentioned above regarding focal depth and magnitude).

Proposal for GMPE change: In view of Paul's comments and the comparison plots, the epistemic uncertainty band on in-slab events should be widened at high frequencies, and re-weighted to better reflect the proposed new Abrahamson et al. GMPE. *Specifically, the upper curve for in-slab events should be increased by a factor of 1.5 at >5Hz, including PGA; the factor would taper from 1.5 to 1.0 as frequency decreases from 5.0 to 1.0 Hz. The representative curves should be re-weighted to place equal weight on the mid and upper curve for higher frequencies – for example, for frequencies up to 1 Hz the weights for low, mid, high would be 0.25, 0.5, 0.25; for frequencies of 5 Hz and greater, including PGA, the corresponding weights would be 0.2, 0.4, 0.4, with a transition of weights taking place between 1 and 5 Hz (eg. For 2 Hz use 0.25, 0.4, 0.35).*

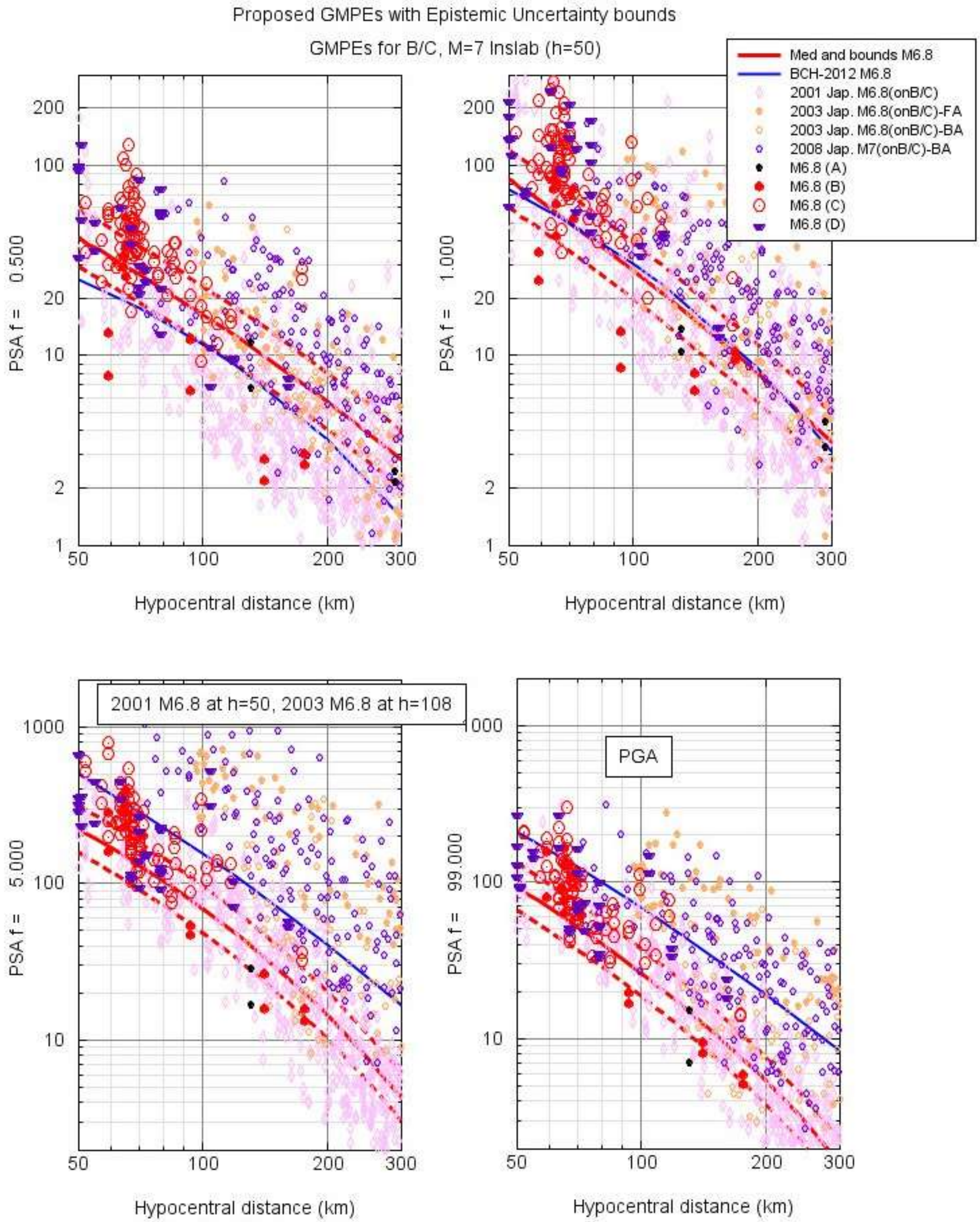

4 - Western Interface Events

Our western interface suite was based on simulations for Cascadia attenuation and site conditions, with the approach calibrated using data from the **M**8.3 Tohoki-oki event (Atkinson and Macias, 2009).

Somerville recommends considering the equations of Zhao et al., 2006, and Abrahamson et al., 2012. In the plot below, we compare Paul's recommended GMPEs to our representative equations, along with **M**9 Tohoku data corrected to B/C site conditions. We focus on **M**9, and on lower frequencies, as this is the most critical for hazard analysis for interface events. At the lowest frequencies (0.2Hz), our GMPEs appear quite conservative relative to Zhao and Abrahamson, and also with respect to the Tohoku data. We note that the Tohoku data match well with our lower equation. At 0.5 Hz our GMPEs are conservative with respect to Abrahamson and the Tohoku data, but less conservative than Zhao. At 1 Hz our GMPEs agree well with Zhao, but show slower attenuation than Abrahamson. At 5 Hz our GMPEs are similar to those of Zhao, but lower than those of Abrahamson. The comparisons suggest that the amount of epistemic uncertainty in our suite is appropriate, but that the weights could be adjusted to take more account of the new Abrahamson et al GMPEs – this involves placing more weight on the lower GMPE at low frequencies, and more weight on the higher GMPE at high frequencies.

Proposal for GMPE change: *For interface events at frequencies 0.5Hz and less, change the weights to 0.4, 0.4, 0.2 for low, med and high, respectively. Retain existing weights for 1.0 Hz. For frequencies of 5 Hz and higher (including PGA), change the weights to 0.2, 0.4, 0.4 for low, med and high, respectively. For intermediate frequencies, a transition in weights can be implemented.*

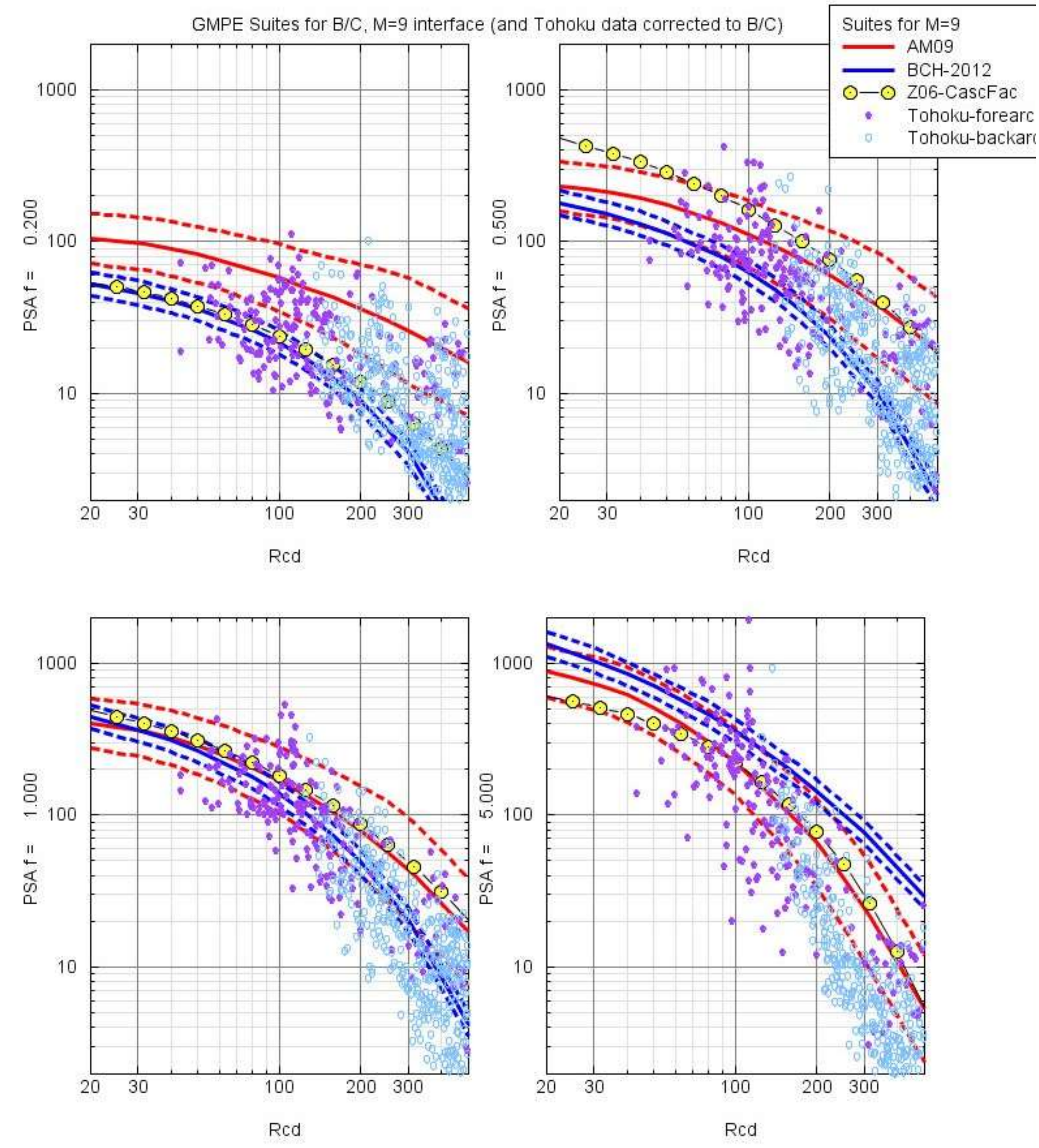

Appendix C: Supplemental Plots

The following pages contain various additional plots of GMPEs that support the discussions made in the white paper.